



FACHHOCHSCHUL - MASTERSTUDIENGANG  
AUTOMATISIERUNGSTECHNIK

---

# Scattering Parameters for Transient Analysis of Shipboard Power Systems

Als Masterarbeit eingereicht

zur Erlangung des akademischen Grades

Master of Science in Engineering

von

**MATTHIAS KOFLER BSc**

Februar 2013

---

Betreuung der Masterarbeit durch

**Prof. (FH) Univ. Doz. Dipl.-Ing. Dr. Karl Heinz Kellermayr**

**Dr. sc. ETH Lukas Graber**



Campus **Wels**

Ich erkläre ehrenwörtlich, dass ich die vorliegende Arbeit selbstständig und ohne fremde Hilfe verfasst, andere als die angegebenen Quellen nicht benutzt, die den benutzten Quellen entnommenen Stellen als solche kenntlich gemacht habe und dass die Arbeit mit der vom Begutachter beurteilten Arbeit übereinstimmt.

Die Arbeit wurde bisher in gleicher oder ähnlicher Form keiner anderen Prüfungsbehörde vorgelegt und auch nicht veröffentlicht.

.....  
Matthias Kofler BSc

Gries am Brenner, 15. Februar 2013

# Acknowledgement

The Center for Advanced Power Systems is a state-of-the-art research facility of the Florida State University and possesses the reputation in doing outstanding research in the field of power systems technology. I have learned a lot throughout my stay at the Center for Advanced Power Systems, with many challenging yet valuable experiences in order to complete this work. This would not have been possible without the help of many people why I want to use this portion of my thesis to mention all those who helped me with my project.

First I would like to thank Dr. Michael „Mischa“ Steuer who has given me the opportunity to accomplish my project in the Power Systems Group and without whom this thesis would not have been possible at all. I would also like to express my gratitude to my supervisor Dr. Lukas Graber who helped me throughout the process obtaining my project and who made working on this thesis very manageable and a great learning experience due to his congenial and easily approachable nature, along with being a pool of knowledge.

I also thank my supervisor in Austria Prof. (FH) Univ. Doz. Dr. Karl Heinz Kellermayr from University of Applied Sciences Upper Austria who was very supportive, helpful and guided me really well from the beginning of this project until its completion. I benefited significantly from the feedback and suggestions of my supervisors not only in technical terms but also in regard to preparing this thesis.

I would also like to thank Dr. William Brey from the National High Magnetic Field Laboratory for providing the equipment and assistance required for doing the measurements needed. Thanks also goes to Dick Benson from the The MathWorks, Inc. for his paramount support and valuable contribution on the modeling topic. Thanks also to everyone else who has been involved in my project in one way or another.

Finally, I would like to thank my parents Elisabeth and Maximilian Kofler for their actively support during my presence as a student.

This work was supported by the United States Office of Naval Research under Grant No. N00014-04-1-0664.

# Kurzfassung

Die vorgestellte Forschung in dieser Arbeit wurde am Center for Advanced Power Systems der Florida State University im Jahr 2012 durchgeführt. Das Thema der Forschung ist das Konzept des zukünftigen “All-electric ship” der United States Navy.

Der primäre Fokus dieser Arbeit beruht auf einem neuartigen Ansatz zur Modellierung und Simulation von elektrischen Systemkomponenten unter Nutzung von Streuparametern (engl. Scattering Parameters) für die Analyse verschiedenster Ausführungen von Erdungssystemen.

In Kapitel 1 und 2 wird eine kurze Einführung in das “All-electric ship”-Konzept und das Thema Erdung von Mittelspannungs-Gleichstrom-Energiesystemen gegeben. In Kapitel 3 wird die Modellierungsmethode basierend auf Streuparametern vorgestellt. Dieser Ansatz ermöglicht die Modellierung von Systemkomponenten wie Leitungen, Sammelschienen, Maschinen, leistungselektronischen Umformern und dem Schiffsrumpf basierend auf generierten bzw. gemessenen Streuparametern für die Entwicklung von Simulationsmodellen. Diese Modelle können anschließend verwendet werden um Simulationsstudien durchzuführen.

Der Ansatz mit Streuparametern ist eine Neuheit im Bereich der Simulation von Energiesystemen. Eingesetzte Simulationsprogramme für die Modellierung von Energiesystemen wie etwa PSCAD/EMTDC oder MATLAB/Simulink erlauben in der Regel keine direkte Integration von linearen Netzwerklöcken basierend auf Streuparametern. Ein N-Tor Block wurde entwickelt, welcher erlaubt Modelle von Systemen und Subsystemen auf der Basis derer Streuparameter in Simulationsprogramme als lineare zeitinvariante Netzwerke einzubetten.

Die Modellumsetzung wird vorgestellt und die durchgeführten Validierungen zeigen sehr gute Modellierungsergebnisse. Als Ergebnis der Forschung können nun Untersuchungen des experimentellen Energiesystems der Purdue University durchgeführt werden zur Unterstützung der Forschung für das “All-electric ship”.

# Abstract

The research presented in this thesis has been performed at the Center for Advanced Power Systems of Florida State University in 2012. Topic of research is the concept for the future All-electric ship of the United States Navy.

Primary focus of this thesis is on a novel approach on modeling and simulation of electrical power system components using scattering parameters for the analysis of different system grounding architectures.

In chapter 1 and 2 a short introduction to the All-electric ship concept and the topic of grounding of direct current power system operated at medium voltage level is given, while in chapter 3 the modeling approach based on S-parameters is presented. This approach allows the modeling of power system components such as cables, bus bars, machines, power electronic converters and the ship hull based on generated or measured S-parameters for the development of simulation models. These models can be used to perform simulation studies.

The S-parameter approach is a novelty in the field of power simulations. Available simulation software packages for power system modeling such as PSCAD/EMTDC or MATLAB/Simulink usually do not allow the direct integration of linear network blocks characterized by S-parameters. A generic N-port block has been developed which allows to embed models of subsystems based on their S-parameter in power systems software packages in the manner of linear time invariant networks.

The model implementation is presented and validation studies have been performed which show very good modeling performance. As a result of the research, investigations can now be performed for studying the experimental power system setup of Purdue University to support the research for All-electric ship.

# Executive Summary

This master thesis is result of an internship at the Center for Advanced Power Systems (CAPS) in Tallahassee, Florida. CAPS is a research facility of Florida State University (FSU) and one of the major partners in the Electric Ship Research and Development Consortium (ESRDC) of the United States Office of Naval Research (ONR). The focus of the research described in this thesis is on the topic of scattering parameters (S-parameters), which are envisaged to support grounding research. The topic of grounding is part of an ongoing research project in the ESRDC with the aim to support the development of next-generation all-electric naval ships. These refer to ships whose power generation, propulsion and auxiliary systems entirely depend on electric power. Further, these ships employ new ship designs and have the ability to make use of advanced weaponry.

Presently, three main systems are being considered which may have application in different future ship types associated to the United States (U.S.) Navy. Of all three architectures defined, the direct current system, operated at medium voltage level (MVDC) is investigated by CAPS. As with any power distribution architecture, there are numerous design considerations that need to be addressed. One issue that has been raised in the design of MVDC power systems is the topic of grounding. This topic is part of the recommended practice for MVDC ship power systems. The system grounding has significant impact on a ship as to personnel safety, survivability and continuity of the electrical power supply. While the grounding practices of AC shipboard power systems are generally well resolved, there is very little literature available and even fewer guidance given how to engineer grounding for DC power systems on ships. Further, there are no approaches to the analysis required to fully understand all the effects of engineered grounding systems on the performance of MVDC systems on ships. Therefore, the research focus in the field of power systems grounding conducted by the ESRDC is on grounding aspects related to this architecture and its conceptual features.

Ongoing research in the ESRDC studies are focused on different grounding schemes of DC shipboard power systems and their impacts on voltage transients, bus har-

---

monics, fault current levels or power loss. One of the research thrusts of shipboard grounding is the transient behavior of the DC bus voltage as a function of the location of a prospective single rail-to-ground fault. Circuit simulation software allows modeling of shipboard power systems and helps to analyze the characteristics of transients for a certain grounding scheme. Recent studies have shown, that in such a fault scenario not only a static response but also high frequency transient phenomena can be observed. The exact shape of these transients depends on high frequency characteristics of all components including the DC distribution bus. Models are required which are suitable to simulate fast transients as they can occur in shipboard power systems with high power density, short line lengths and low damping characteristics. It has shown that simulations models based on lumped elements have only limited capabilities to accurately model high-frequency transients. Such models do not include effects of travelling wave propagation and reflection. A completely new approach had to be developed.

Following these studies the characterization of power systems components based on scattering parameters (S-parameters) has been initiated. The S-parameters approach is not common in power systems and to the author's knowledge a novelty in the field of power simulations. Therefore, the aim is to develop models of systems and subsystems and determine their S-parameters. In particular this work focuses on embedding S-parameters in models of shipboard power systems with emphasis on the implementation in Simulink/SimPowerSystems. Simulation software packages routinely used in ESRDC activities for shipboard power systems simulations such as PSCAD/EMTDC or MATLAB/Simulink do not allow the direct integration of linear network blocks characterized by S-parameters. This is in contrast to software packages commonly used for high-frequency engineering in which S-parameter blocks are typically available.

A generic N-port block has been developed which allows to embed models of subsystems based on their S-parameters in power systems software packages assuming linear time invariant (LTI) networks. Validation of this implementation has been conducted using Agilent Advanced Design System (ADS). LTI networks have been defined by circuits using passive lumped elements. The same circuits have been implemented in SimPowerSystems by their S-parameters and the step response recorded. An overlay of the results shows a perfect agreement. It has been shown that the accuracy of the S-parameters implementation is qualified for high-fidelity power systems simulations.

Purdue University, another member of the ESRDC, designed and built a small-scale

---

testbed to study the performance of different grounding schemes proposed for MVDC power systems. A complete S-parameters characterization of the power electronics components incorporated has been conducted. The measurements were carried out in collaboration with the National High Magnetic Field Laboratory (NHMFL) by means of a 2-port vector network analyzer (VNA). MATLAB tools and scripts have been established which support the overall S-parameters approach. As a result of the research, investigations can now be performed for studying the experimental power system setup of Purdue University to support research for AES.

# Contents

<b>1</b>	<b>All-Electric Ship Concept for Future’s Naval Warfare</b>	<b>1</b>
1.1	All-Electric Ship . . . . .	1
1.2	Electric Power Distribution Architectures for Future Naval Ships . . .	6
1.3	Shipboard Grounding Schemes . . . . .	8
<b>2</b>	<b>Grounding Schemes for MVDC Power Systems</b>	<b>9</b>
<b>3</b>	<b>Modeling of Power Systems Components</b>	<b>14</b>
3.1	General Aspects of Modeling . . . . .	14
3.2	S-Parameters as Modeling Approach for Multiport Networks . . . . .	16
3.3	Measurement of Scattering Parameters of an N-port Network . . . . .	21
3.3.1	Vector Network Analyzer . . . . .	21
3.3.2	Multiport Measurement by Means of a 2-Port Vector Network Analyzer . . . . .	24
3.3.3	Measurement of Purdue’s Small-Scale Testbed Components . . . . .	27
3.4	Model Implementation and Validation . . . . .	31
3.4.1	Model Implementation . . . . .	31
3.4.1.1	Rational Function Fitting . . . . .	31
3.4.1.2	Generation of Transfer Function Blocks . . . . .	34
3.4.1.3	Circuit Level Model Implementation . . . . .	35
3.4.2	Model Validation . . . . .	37
3.5	Circuit Simulations . . . . .	40
3.5.1	Transmission Line Model (3-PI-Section) . . . . .	40
3.5.2	DC/DC Converter Model . . . . .	42
3.6	Solver Settings and Pitfalls . . . . .	44

---

<b>4 Conclusion</b>	<b>47</b>
<b>List of Figures</b>	<b>50</b>
<b>List of Tables</b>	<b>53</b>
<b>List of Abbreviations</b>	<b>54</b>
<b>Bibliography</b>	<b>56</b>
<b>A Archiving</b>	<b>61</b>
<b>B MATLAB Tools</b>	<b>63</b>
B.1 Main GUI . . . . .	63
B.2 Rational Fitting for S-parameter Transfer Functions . . . . .	64
B.3 Visualization of S-parameter data . . . . .	66
B.4 Generation of Touchstone <sup>®</sup> -File . . . . .	68
B.5 Assembling of the N-Port S-Matrix . . . . .	70
<b>C S-parameters Model Description</b>	<b>72</b>
<b>D Multiport Characterization using a 2-Port Network Analyzer</b>	<b>76</b>
D.1 3-Port Network Measurements . . . . .	76
D.2 4-Port Network Measurements . . . . .	77
D.3 5-Port Network Measurements . . . . .	78
D.4 6-Port Network Measurements . . . . .	79
<b>E Documentation of the Master Thesis on CD</b>	<b>80</b>

# 1 All-Electric Ship Concept for Future's Naval Warfare

## 1.1 All-Electric Ship

In recent years, the U.S. Navy began to reconsider the concept of traditional naval ship systems as a consequence of growing costs and military capabilities with the goal to make ships more efficient and affordable by exploring new and more reconfigurable system architectures.

Conventional naval ships employ geared mechanical drive systems for propulsion. These ships host two separate sets of engines to provide the necessary energy for ship propulsion and service loads [1]. One set of engines is directly-linked to the mechanical propulsion system since a large amount of installed power is dedicated to the propulsion [2]. Typically this set contains two pairs of gas turbines as the prime movers whereby each pair is connected to a large common reduction gearbox to reduce the engine's high rotational-speed and to permit the operation of the propeller at lower rotational speeds. For survivability reasons one drive train must be located forward and the other aft. As a result, long line shafts of the propulsion system are running through the ship to connect the gearboxes and rotate the propellers. Furthermore, the propellers location defines the centerline of the shaft lines and hence the vertical position of the prime movers [3]. The required location as well as the size and number of the installed machinery of the mechanical propulsion system are considerable factors which reduce the internal space available for equipment other than propulsion. These prohibit efficient use of capacity, and restrict ship designers in their design flexibility. It might be fair to say the rest of the ship needs to be arranged and designed around these set of engines instead of creating a customized propulsion system for the ship. A second set, typically including three gas turbines or diesel generators, is connected to smaller auxiliary generators to operate all the electrically powered equipment on these ships [4].

It is a fact, that naval warships operate relatively little time at maximum speed [5]. The majority of the installed power generation is locked in the propulsion system and not available for non-propulsion loads. The overall efficiency of these ships can suffer due to the inefficiency of the propulsion prime movers at low operation speed [4, 5]. These facts have an impact to increased fuel consumption, increased operation costs, system efficiency and mission flexibility.

Over the recent decades electric-drive technology has been considered and introduced and finally accepted as possible alternative to mechanical drive systems. With the beginning of the eighties, ships built with electrical propulsion systems have become more popular and are found today in many types of ships such as cruise liners, ice-breakers and amphibious assault ships. Electric propulsion systems, eliminate the need of a mechanical link between prime movers and propeller. Propulsion shafts can be shorter and do not need to be aligned any longer [6]. The missing physical connection enables cross-connecting between power generation and power operated ship systems. This provides ship designers a considerable amount of arrangement flexibility to place the gas turbines where they will optimize space, weight and balance of the ship without interfering with ship mission equipment. The introduction of electric propulsion equipment into naval ships resulted in a considerable increase of the electric power level, since usually the electric propulsion represents the most demanding electrical load on the ship [7]. Furthermore, in future the U.S. Navy is moving towards more unconventional mission weapon systems, weapon launchers and sensors with higher electrical power requirements such as high energy Laser weapon, electro-magnetic gun, electro-magnetic assisted aircraft launcher or Radar systems to name just a few. They are gaining increased importance due to change in the philosophy of naval warfare [8].

To meet the requirements of changing trends and demands regarding to power, improved mission capabilities along with superior system efficiencies and decreased operating costs in future, the U.S. Navy is investing substantial in exploring ways to power so-called All-electric ships (AES) [1]. This next-generation ship concept is being mapped out in a program by the U.S. ONR<sup>1</sup> known as the Next-Generation Integrated Power System (NGIPS). It aims at to make more efficient use of on-board power by incorporating the knowledge learned from utilization and development of the Integrated Power System (IPS) which has been developed by the U.S. Navy between 1992 and 2006 [9]. Other than traditional warships the AES refers to a ship whose power generation, propulsion and auxiliary systems entirely depend on

---

<sup>1</sup><http://www.onr.navy.mil/>

electric power (as opposed to mechanic, hydraulic, steam or compressed-air powered systems). The IPS is evolved as to be the most appropriate solution to overcome the increasing power demand and to fulfill all electrical needs of a future naval warship [8, 10].

Unlike traditional power system configurations, which have dedicated power sources for propulsion and ship electrical power generation (also known as Segregated Power System), the IPS architecture features electric-drive propulsion and is designed to produce power for both propulsion and ship service systems and enables the development of affordable configurations for a wide range of ship applications such as submarines, surface combatants, aircraft carriers, amphibious ships, auxiliary ships, sealift and high value commercial ships by providing a common pool of electrical power throughout the ship. Combining propulsion and electrical ship service system into a single power system not only reduces the total number of prime movers but also provides a considerable increase of overall system efficiency compared to an equivalent mechanical drive design [4]. All prime movers in an IPS are coupled to generators which are capable to produce more than the maximum peak power for the propulsion but less than the sum of peak power of all electric loads. On top of this the IPS allows to release and reallocate the large amount of power which is dedicated to the propulsion to accommodate combat systems for any given operating condition, especially when high-speed propulsion is not an operational requirement [6].

The IPS architecture can be implemented in Zonal Electrical Distribution (ZED) structure [8]. The design method of dividing the ship into multiple electrical zones allows to isolate each zone from each other and enables the ship to withstand a certain level of damage. On the power-level, prospective electrical faults and their propagation can be localized and controlled in a more efficient fashion. Loads outside two adjacent damaged zones do not see an interruption of power [11]. This added robustness together with the ability that electrical power (contrary to mechanical power) can be relatively easily redistributed to loads of higher priority in battle mode or, in case that damage occurs on the ship, to undamaged propulsion systems, service or mission critical combat systems. This results in a substantially increased flexibility in ship design re-configurability and combat survivability.

Although the advances in ship technologies and the scheme of power design offers anticipated benefits in many respects and provides ship designers opportunities to meet the individual needs and operational requirements of different ship types easier, this architecture makes the shipboard grid structure rather complex due to multiple in-

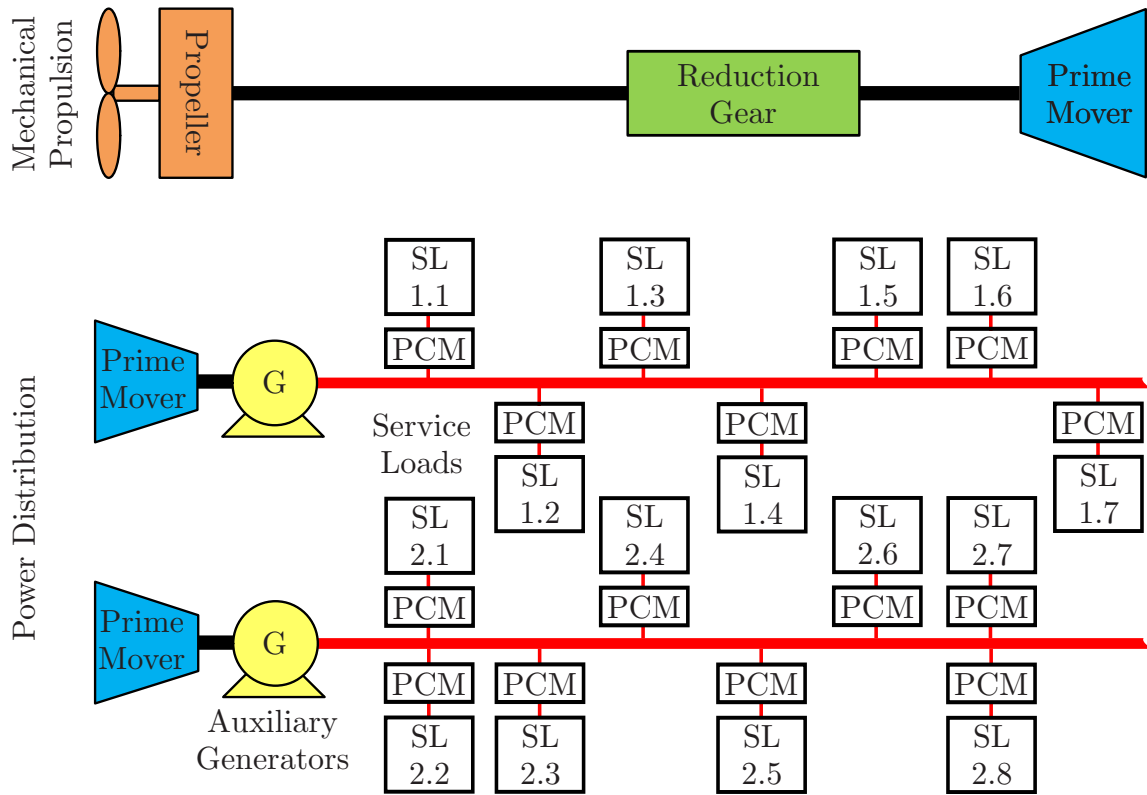
teracting (sub)systems. Impacts on the ship equipment are more serious in case that a fault occurs as a consequence of higher voltage levels [10]. Electric-drive propulsion equipment might be larger and heavier compared to equivalent mechanical-drive devices. As with any industrial product, the component-level technology is moving towards becoming smaller and lighter by being more energy efficient. It is expected that size and weight of electric-drive systems will come down over time to dimensions comparable to mechanical drive systems. Nevertheless the merits of the integrated electric-drive propulsion such as fuel savings can offset the size and weight drawback already today [1].

Figure 1.1 compares a conventional ship design with a design based on IPS. Although this figure does not correspond to any real ship's one-line diagram (multiple generators, motors and conduction paths for reliability and survivability), it provides a basic understanding of the essential differences of a power system configurations including mechanical ship propulsion compared to an integrated electric architecture. Even if commercial ships are already using electric propulsion the concept and development of a next generation naval ships based on AES is still in its infancy [1]. The utilization of large power level generation and distribution on ships with their severe space constraints, poses new multidisciplinary challenges in ship design and manufacturing.

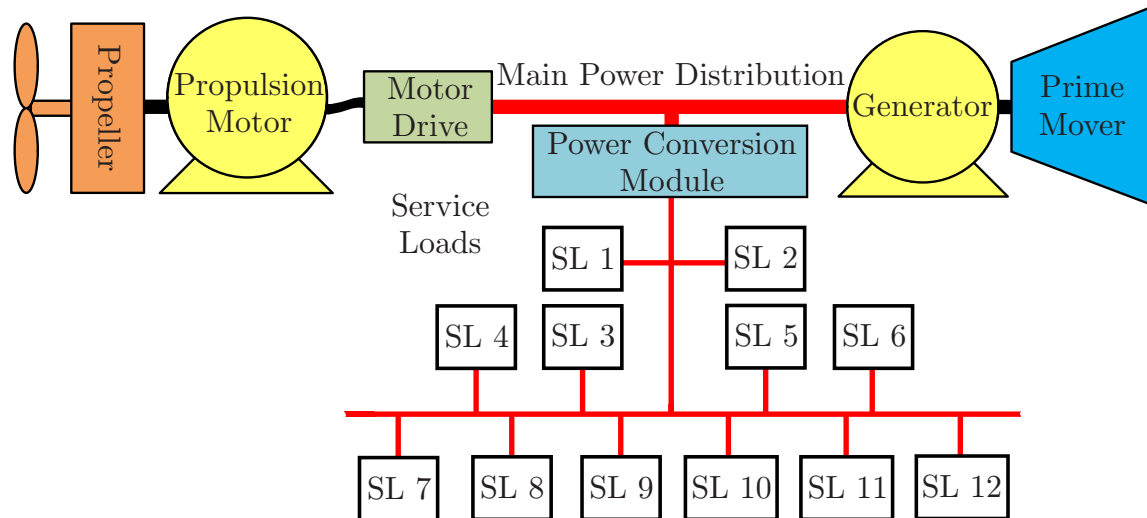
As there are many uncertain parameters in many respects which need to be addressed, the U.S. ONR established the ESRDC<sup>2</sup>. ESRDC is a consortium of eight individual research institutions with fundamental knowledge in the field of power systems technology and focuses on research in electric ship concepts. These institutions are dedicated not only to furthering research in electric ship and other advanced electric technologies, but also to address the national shortage of electric power engineers by providing educational opportunities.

---

<sup>2</sup><http://www.esrdc.com/>



(a) Conventional Ship Design showing prime movers, auxiliary generators, service loads (SL) and power converter modules (PCM)



(b) Electric Propulsion with Integrated Power

Figure 1.1: Simplified shipboard power system comparing a conventional design (above) with a design based on IPS (below) [6, modified]

## 1.2 Electric Power Distribution Architectures for Future Naval Ships

The selection of power system architecture for a ship primarily depends on the specific requirements of the ship under design and attached to this on factors such as quality, efficiency, survivability and reliability desired. Currently three main systems are being considered which may have application in different future ship types associated to the U.S. Navy: Medium-Voltage AC (MVAC), High-Frequency AC (HFAC) and Medium-Voltage DC (MVDC). Whereas the first two architectures are proposed for near term applications, is the Medium-Voltage DC (MVDC) considered to be the most appropriate power system architecture for future's naval All-electric ships (Figure 1.2) [5].

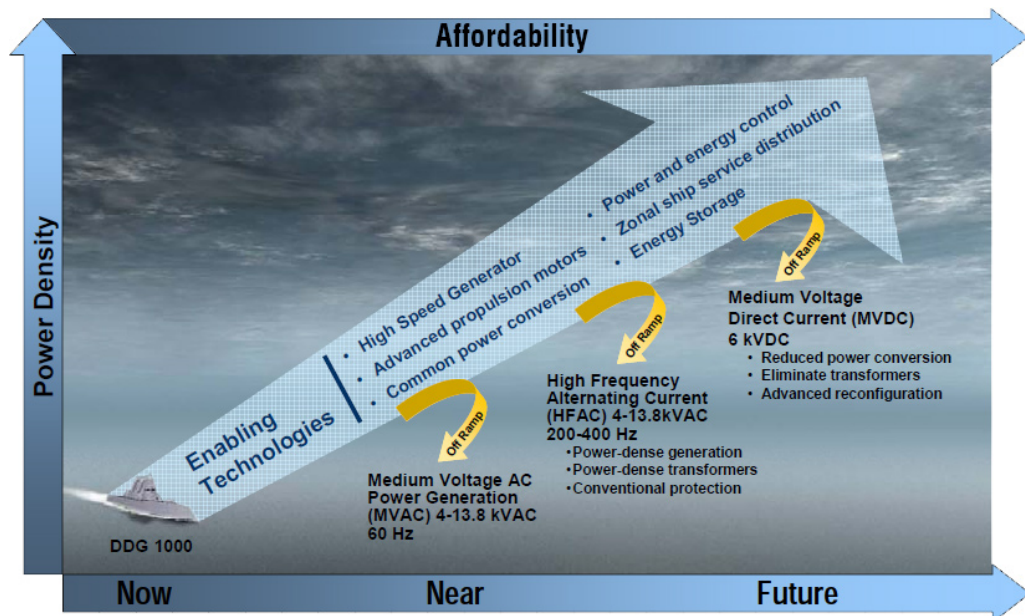


Figure 1.2: Next Generation Integrated Power System (NGIPS) Technology Development Roadmap. The DDG-1000 Zumwalt Class destroyer is the poster child for the U.S. Navy to shift to all-electric ships. [5, modified]

**Medium-Voltage AC (MVAC):** In an MVAC integrated power system, power is generated and shared by means of a 3-phase distribution bus at conventional power frequency of 60 Hz at one of three standard voltage levels (4.16 kV, 6.9 kV or 13.8 kV). The MVAC architecture is appropriate for ships where high power density is not a requirement [5]. The MVAC architecture is well investigated by the shipbuilding community induced due to the similarity to land-based (i.e. terrestrial)

AC power distribution systems and thus can be deployed in the ship with limited development effort.

**High-Frequency AC (HFAC):** Unlike the MVAC integrated power system, power is generated at a fixed frequency at or above 200 Hz rather than 60 Hz but less than 400 Hz and hence referred to as the high frequency architecture. HFAC is an intermediate step towards the MVDC architecture and for ships with high power density requirements. On one hand it provides several advantages compared to MVAC such as a reduction of size and weight of transformers and rotating machinery, improved acoustic performance or lower harmonic distortion. On the other hand, the higher frequency also introduces several challenges such as high number of poles being required for generators. Prime movers are restricted to specific operating speeds [5].

**Medium-Voltage DC (MVDC):** The MVDC integrated power system is the target NGIPS architecture to meet the high power density requirements of future surface combatants and submarines. The primary difference on system-level compared to an (HF)AC power system is that power is generated as AC, but distributed as DC power through out the ship. Consequently a couple of conceptual features come along with this architecture. The prime movers speed is fully decoupled from the frequency of the main distribution bus which enables the possibility to optimize the generators for each type of prime movers without gears. Engineering concerns (e.g. cable installations) with respect to electromagnetic interference (EMI) and electromagnetic compatibility (EMC) present with HFAC architecture are reduced. On system-level the DC system is simpler, since many conversion steps are avoided. Each step conversion causes losses and potentially reduces reliability of the system. Overall the MVDC architecture is predicted to provide the highest payoff by promising highest capabilities at the least total cost of ownership [12]. However, the application and conceptual changes of the MVDC architecture make this the technically most challenging one of all three architectures defined [5].

The pros and cons of the integrated power system architectures are described more detailed in [5].

The architectures mentioned above have in common, that the choice of appropriate grounding schemes is of utmost importance for the performance of the power system.

### 1.3 Shipboard Grounding Schemes

The grounding strategy of an electrical shipboard power distribution system is a major aspect since the primary objective is personnel safety, availability and continuity (reliability) of the electrical power supply in case of a system fault. Traditionally, literature and especially established engineering practices, distinguish between ungrounded, impedance grounded (high or low impedance) and effectively grounded power systems. The different grounding schemes arise from the characteristic of the connection between the current-carrying conductors and ground. Grounding in this context considers the ship hull to be on ground potential. Strictly speaking there are no ungrounded systems since there is always some degree of parasitic coupling to ground present. Therefore, ungrounded systems are also understood as parasitically or not intentionally grounded systems. For ships unintentionally or high-impedance grounding schemes are preferred since those allow to continue operation of all equipment throughout the ship in case of a single-rail-to ground fault (without clearing the first ground fault exists) [13]. But these grounding schemes come with their own set of issues. One problematic issue arises when locating such a fault since those do not provide considerable fault currents for tracing fault location [14]. This may be critical since an additional fault on the opposite rail under a faulted condition causes a full short circuit. In [14] a novel approach for locating a fault is presented and classical available fault location techniques are discussed.

The established practices of grounding for shipboard electrical power systems [15] still rely on rather simplified analytical approaches which have primarily been established and validated for terrestrial power systems [16]. An overview on most common grounding schemes as well as their performance with respect to system overvoltages and ground currents can be found in [16].

While the grounding practices of AC shipboard power systems are generally well resolved, there is very little literature available and even fewer guidance given how to engineer grounding for DC power systems on ships. Capacitive, resistive, and inductive grounding have specific characteristics which need to be carefully studied. To establish a deliberate connection to ground provides a predictable operating point and reduces voltage stress seen by the system components. Also the location of the engineered grounding point has substantial impact to the performance of the power system during normal operation and during faults [13].

Therefore, the research focus in the field of power systems grounding conducted by the ESRDC is on grounding aspects of MVDC power distribution systems.

## 2 Grounding Schemes for MVDC Power Systems

Unlike terrestrial distribution systems, shipboard power systems carry a couple of unique features such as the presence hazardous conditions during missions, high requirements for reliability and the ability for continuity of operation during certain fault scenarios, low damping properties and significantly high power density due to short cable lengths, wide spread use of power electronics devices and non-linear loads. Furthermore, the power distribution system of future electric ships will be likely different from terrestrial power systems and conventional AC shipboard power systems. Its architecture is MVDC and features a single service line for propulsion and service loads. Beside the increased reconfiguration options to support maximum capability on the ship at all times, it results in an increased adoption of power electronics and increased power demands due to electric propulsion system and pulsed loads [17]. The conceptual innovation attached to the MVDC distribution system raises numerous design considerations which need to be addressed in future. One key issue following the recommended practice for MVDC electrical shipboard power systems and the unique features mentioned above is the grounding strategy. The system grounding scheme has significant impact on many facets of operation on the ship [18]. A detailed comparison between shipboard power systems and terrestrial systems is provided in [17].

Ongoing research in the ESRDC studies different grounding schemes of DC shipboard power systems and their impacts on voltage transients, bus harmonics, fault current levels or power loss. In [19] and [18] different grounding schemes and their impact to the ships power system as a function of the location of a prospective single rail-to ground fault have been studied and the performance compared. The grounding schemes under consideration are: grounding at the DC midpoint ( $V_{mid}$ ), grounding at the neutral point of the generator ( $V_n$ ) and an ungrounded system. In this context the ship hull is assumed to be on one single ground potential.

Figure 2.1 shows a simplified DC power system of a more complex MVDC shipboard

power system topology often found in literature. The simplification is argued from a system ground prospective to be fully sufficient to gain insight into the grounding aspects related to the proposed grounding schemes.

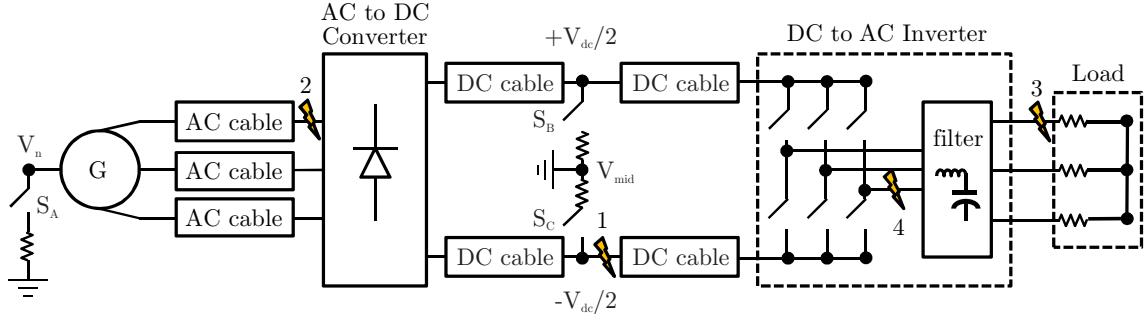


Figure 2.1: Simplified DC distribution system showing four different locations for potential faults (arrow 1 to 4) [19]

The system under study consists of a 3-phase generator on the AC side representing the total generation available in the power system, a diode rectifier, a DC distribution bus („DC cable“) and a 3-phase inverter to feed power into a resistive load. Also the presence of AC power cables from the generator is taken into account. The zigzag symbols indicate possible locations where single rail-to-ground faults can occur. The switches  $S_A$ ,  $S_B$  and  $S_C$  are used to change the location of the engineered grounding point and hence to change from one grounding configuration to another. To illustrate on scenario the evaluation is continued by considering the presence of a single ground fault at the negative DC rail ( $S_B$  and  $S_C$  closed,  $S_A$  open). It has shown that the main distribution bus not only experiences a voltage offset but also a transient phenomena takes place.

The steady state voltage with respect to ground of the positive rail assumes twice the voltage present before the fault. The negative rail potential assumes ground potential. Even if the DC bus is affected by means of a shift of the steady-state voltages, the differential voltage (rail-to-rail voltage) level remains unchanged as in normal operating conditions and thus the loads remain unaffected as long as they are isolated from ground. However, the transients on both DC bus rails cannot be ignored. They not only occur in the event of a fault, but are potentially also initiated by switching events of circuit breakers or power electronics (e.g. IGBTs). By means of a parametric study it turned out that the transients initiated by the fault significantly depend on certain parameters throughout the system such as stray capacitances to ground or the load. One of the finding refers to the accuracy

of cable models which have significant influence to the amplitude and oscillation frequency of voltage transients. The case studied in Figure 2.2 shows a dominant oscillation frequency of approximately 0.35 MHz. These transient overvoltages may stress affected equipment and hence shorten the lifetime. In worst case the sum of temporary excess of the voltage, the rate of rising as well as the reversal in voltage polarity can be severe and cause permanent damage to insulation and power electronics.

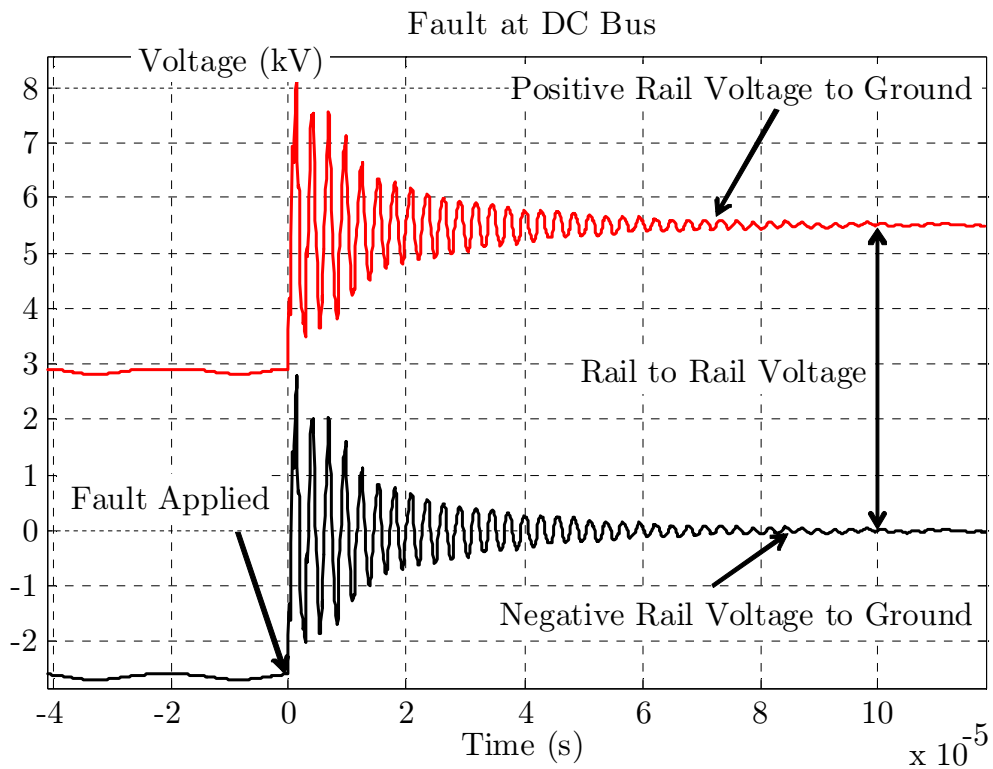


Figure 2.2: Transient phenomena and system offset for a high grounding impedance [19]

In [20] the importance of accurate cable models has been studied more detailed. Lumped element models are commonly used for power simulations. Other than distributed parameter line models those are more practical to implement. To validate the quality of these models, three different cable models of a medium voltage power cable usually used in domestic distribution systems have been established. The cable is predicted to be suitable for shipboard power systems as well and hence chosen to show the process of validation. The first two are single-phase transmission line models based on lumped elements. The first model consists of a single PI-segment. For the second model, a cascade of three PI-segments is selected. The third model

tested is a distributed RLC traveling wave model, available in the software package PSCAD<sup>1</sup>. According to [21], there are essentially two different types of models for transmission lines. One is based on uniformly distributed parameters and the second is based on lumping these parameters into a lumped element equivalent circuit (e.g. Gamma or PI forms). The parameters (resistance, inductance and capacitance) of a transmission line are uniformly distributed along the line. To determine an accurate transient behavior of a transmission line, an exact representation of distributed parameters is required. An approximate model of a distributed parameter line model can be obtained by cascading multiple identical PI segments. The accuracy of lumped parameter approximation depends on the line length and highest transient frequency component involved. Therefore representation of transmission lines may require several line segments to achieve sufficient accuracy. A single PI-segment line model is appropriate for modeling short transmission lines or when the frequency range of interest is limited around the fundamental frequency. A more accurate modeling of high frequency characteristics of a cable can be obtained by cascading several identical single PI-segments. Latter can be derived by dividing the basic PI line model into the number of segments required. However, these three models have been compared to the measurement performed utilizing the approach of scattering parameters (S-parameters) characterization by means of a vector network analyzer (VNA). The proposed measurement method has been selected since it allows the characterization of linear elements (as the cable can be assumed) over a wide frequency spectrum. The comparison of the results has shown that simulations based on simple lumped element models have limited capabilities to accurately model and represent high frequency transient phenomena due to traveling wave propagations and reflections in cables. In comparison to the PI section line model, the distributed line model and S-parameter measurements represents wave propagation phenomena and line end reflections with much better accuracy. Referring to this, the authors conclude, that the proposed method of using S-parameters is an efficient and accurate way to characterize any linear device within a particular frequency range of interest.

Based on these studies, it is envisaged to develop physics-based Finite element models (FEM) and to extract their S-parameters. The modeling of (complex) geometry structures as it is the ship hull or electrical power system components such as cables, bus bars, electrical machines or power electronic converters are being considered to be modeled. The integration of such models into grounding-related power system

---

<sup>1</sup><https://hvdc.ca/pscad>

simulations may results in increased quality of simulation results. Purdue University another member of ESRDC built a small-scale testbed in order to conduct grounding studies of DC shipboard power systems. It is scaled in dimensions as well as voltage and power scaled. The experimental setup represents a MVDC system (of reduced complexity) which is considered for shipboard NGIPS for future naval vessels. It provides the opportunity to evaluate system performance under grounded and ungrounded configurations. It is planned to perform S-parameter measurements of components which are integrated in this physical testbed. Figure 2.3 shows the common components of a simplified DC power distribution system considered as multiport (N-port) networks. To the author’s knowledge the S-parameter approach is a novelty in the field of power simulations. Available simulation software packages for power system modeling such as PSCAD/EMTDC or MATLAB/Simulink<sup>2</sup> usually do not allow the direct integration of linear network blocks characterized by S-parameters. These facts initiated this project. The aim is to develop a generic N-port block which allows to embed models of subsystems based on their S-parameter in power systems software packages in the manner of linear time invariant (LTI) networks. Furthermore, the S-parameters of the power devices included in the experimental setup of Purdue University shall be determined for further investigations.

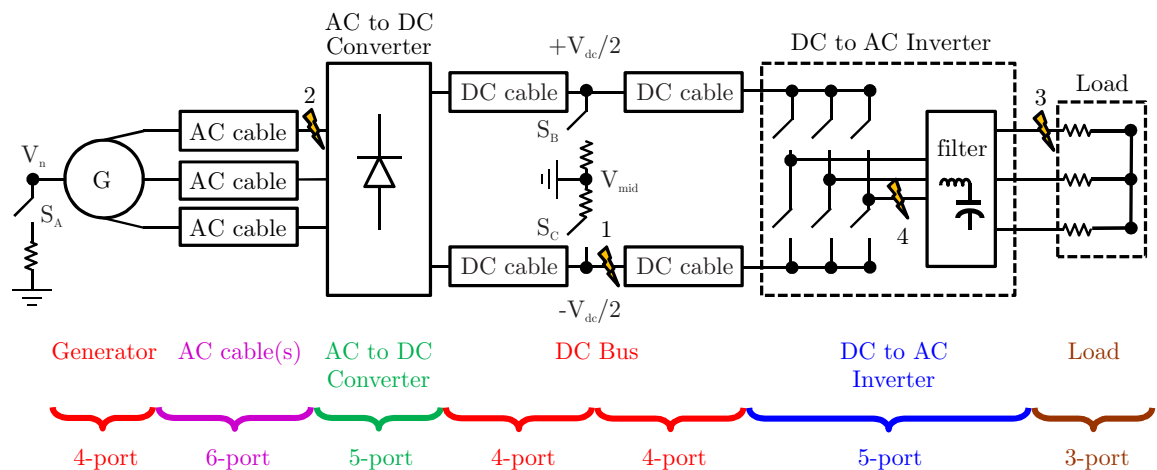


Figure 2.3: Common components of a simplified DC distribution system considered as multiport (N-port) networks. Ship hull is treated to be a perfect conductor. [19, modified]

<sup>2</sup><http://www.mathworks.com>

# 3 Modeling of Power Systems

## Components

### 3.1 General Aspects of Modeling

Grounding of MVDC power systems requires significant investigations to fully understand all the effects related. To perform such investigations mathematical models and simulation tools have proven to be efficient and very cost effective. Simulation studies are a major and unavoidable part within the progress of developing technologies. It enables to study design alternatives of a system and their impact on certain key parameters focused on without carrying out experiments or building hardware prototypes. The potential of guiding early stage designs and the detailed analysis of design and all the effects related allows to reduce the risk and costs of early decision. Even so, the accuracy of simulation results strongly depends on the accuracy of the models being used for the simulation.

A power system is considered as electrical network and for those networks many modeling concepts exist for its static state as well for its dynamic behavior. There are two basic different approaches to model a system. Derivation of the fundamental equations to describe system behavior from the law of physics etc. is called as „White Box“ approach. On the other side it is possible to find a model description exclusively using experiments and measured input-output data. This approach to modeling is called experimental system identification or „Black Box“ approach. For modeling of electrical, mechanical and control systems there exists a well developed body of knowledge especially for linear systems and in particular for LTI systems. Such systems can be modeled and described in the time domain by linear differential equations and in the frequency domain by concepts such as transfer functions. Fourier transform allows to transfer from time domain to frequency domain representation. In the other direction the inverse Fourier transform can be used.

An ongoing research project in the ESRDC studies the impact of different grounding

schemes of MVDC based on the mathematical and physical prototype models. Of special interest are the dynamics, the transient behavior of the system if a single rail-to-ground fault occurs. The exact shape of these transients depends on high frequency characteristics of all components including the DC distribution bus. Time domain simulations typically employ lumped element models which makes it difficult to represent the distributed nature of the system to be modeled. Transmission lines are by their nature distributed parameter systems. These can be modeled based on theory and analytical approaches such as Bergeron's traveling wave method [22]. Due to the complexity this might not be applicable for power electronics components as they are included in the power system being considered. It is assumed to be critical and challenging to successfully build an extensive model which represents their high frequency characteristics and propagation behavior over a wide frequency range required to observe transient phenomena. Here, a measurement-based modeling approach is taken into consideration to be an alternative. S-parameters provide a concept for modeling linear electrical networks.

However, a characterization of power electronic devices (PED) based on S-parameters measurements is not common since PED such as rectifiers, DC/DC converters or 3-phase inverters are strongly nonlinear systems due to their use of semiconductors and control circuitry. The main source of nonlinearity is caused by switching semiconductors in the PED. The switching frequency of PED in the megawatt range is typically in the lower kHz-region. According to the theory of the S-parameters, which represent the linear electrical behavior of any electrical linear time-invariant network, the proposed technique is not applicable for the characterization of such PED. However, the oscillation frequencies of voltage transients in ship power systems are expected and established in previous studies to be around two orders of magnitude (or even more in case of diode rectifiers) higher than the switching frequencies of PED. This fundamental fact introduces the hypothesis, that the probability is low that component related switching events coincide with a transient voltage caused by other reasons than semiconductor switching. Consequently, it is assumed that PED behave linearly for the time period of prospective voltage transients. Even if the addressed events coincide it is supposed that switching operations do not substantially impact the amplitude and oscillation frequency of voltage transients.

This chapter provides the necessary theory to the S-parameters proposed in the previous section as well as the steps needed to implement S-parameter measurements in a circuit simulation.

## 3.2 S-Parameters as Modeling Approach for Multiport Networks

The derivation of a corresponding equivalent lumped-element model to an electrical system or device might not always be readily achievable, since the electrical design and functionality can be complex and many aspects are unknown. A system of which the system response is known if it receives a specific input (e.g. step excitation), but not its inner functionality is termed as “Black Box”. System description based on network parameters is a useful method for representing the external behavior of such a system without any regard to the inner setup in a very convenient way.

S-parameters are widely used to characterize any LTI network in the frequency domain. These parameters are central in microwave theory and hence extensively used for characterization, modeling, and design of radiofrequency and microwave devices since they are easier to measure at higher frequencies than alternative network representations such as impedance parameters (Z-parameters) or admittance parameters (Y-parameters) [23, p. 50]. The latter require measurements to be performed in open circuit and short circuit configuration which are in practice extremely difficult to achieve at high frequencies since both conditions are affected by either a parasitic capacitance (open-circuit) or a parasitic inductance (short-circuit) [24, p. 168]. Furthermore such conditions can lead to circuit oscillations and instability of the devices under test (DUT) and in worst case in the destruction of the device. At lower frequencies these alternative network representations are equally applicable and the use of S-parameters would not be essential. However, S-parameters measurements bypass that impact at high frequencies by always connecting all unused ports by a well-defined, in most cases standard  $50\ \Omega$  termination. Although S-parameters are typically associated with high frequencies, the proposed concept is valid for any frequency.

A multiport network as shown in Figure 3.1, often termed as N-port, is an arbitrary electrical network which theoretically may have any number (N) of ports. A network port is understood as a pair of terminals and can be explained as the point at which an electrical signal either enters or exits the network. Whereas impedance and admittance matrices attempt to describe the relation between the total voltages and currents of a network, existing at all ports present, the scattering matrix (S-matrix) describes the transmission and reflection characteristics of the network in terms of incident and reflected waves at all ports present [23, p. 50]. In other words, total voltages and currents are considered to be in the form of travelling waves.



and can be reduced to a single equation using the matrix representation

$$\mathbf{b} = \mathbf{S} \mathbf{a} \quad (3.2)$$

with  $\mathbf{a}$  and  $\mathbf{b}$  being the waves traveling towards and outwards the network at all ports present, and  $\mathbf{S}$  denoting the S-matrix. Thus both,  $\mathbf{a}$  and  $\mathbf{b}$  are vectors of dimension  $N \times 1$  whereas  $\mathbf{S}$  is a  $N \times N$  matrix containing  $N^2$  elements, where  $N$  is the total number of network ports. Considering a single port of a  $N$ -port network, generally denoted as the  $i^{th}$ -port,  $a$  and  $b$  referring to [26] are defined in terms of the total voltage and current as

$$a_i = \frac{V_i + Z_i I_i}{2\sqrt{|\operatorname{Re} Z_i|}} \quad (3.3)$$

$$b_i = \frac{V_i - Z_i^* I_i}{2\sqrt{|\operatorname{Re} Z_i|}} \quad (3.4)$$

and called power waves, where  $V_i$  and  $I_i$  are the terminal voltage across and terminal current through the  $i^{th}$ -port and  $Z_i$  is the reference impedance as seen from the  $i^{th}$ -port or in other words, the impedance connected to the corresponding port. Physically treated,  $a_i$  and  $b_i$  are normalized incident and reflected peak voltages and closely related with power. Accordingly  $|a_i|^2$  and  $|b_i|^2$  represent the power traveling toward and back the  $i^{th}$ -port of the network.

All the elements of the S-matrix (referred to as S-parameters)

$$\mathbf{S} = \begin{pmatrix} s_{11} & \dots & s_{1N} \\ \vdots & \ddots & \vdots \\ s_{N1} & \dots & s_{NN} \end{pmatrix}$$

are a function of frequency as well of the locations of the reference or terminal planes  $t_x$  (define the network ports) and defined for steady-state stimuli in terms of a set of  $N$  reference impedances. Consequently,  $\mathbf{S}$  becomes a matrix  $N \times N \times M$ , representing  $M$   $N$ -port S-parameters, where  $M$  is the total number of frequency points. The expressions (3.3) and (3.4) are defined for the use of any arbitrary characteristic impedance, for the simple reason that under general conditions the reference impedances are not required to be purely resistive. Different impedances  $Z_i$  can be used at each port, even complex. In conjunction with this, the notion generalized power wave is used. S-parameters are most commonly given with reference to a  $50\Omega$  test environment, meaning that  $Z_i$  is a real-valued positive impedance, typi-

cally denoted as  $Z_0$  and identical at all ports present. In this case the previously defined power waves are equal with the expressions with those known in literature as traveling waves [26].

Considering S-parameters, each element of the main diagonal of  $\mathbf{S}$  is a reflection coefficient of a corresponding port when the other ports are terminated by perfect matched loads and contains the ratio of amplitude of reflected and incident wave of a certain frequency [28, p. 90]. Conversely, the off-diagonal elements are transmission coefficients between the ports containing the ratio of amplitude of transmitted and incident wave [28, p. 90]. The related requirements prior are applicable as well. Following this, S-parameter of the main diagonal can be determined as

$$s_{ii} = \left. \frac{b_i}{a_i} \right|_{a_k=0 \forall k \neq i} \quad (3.5)$$

with  $b_i$  being the reflected power wave amplitude and  $a_i$  being the incident power wave amplitude at the  $i^{th}$ -port. The off-diagonal S-parameters can be found as

$$s_{ij} = \left. \frac{b_i}{a_j} \right|_{a_k=0 \forall k \neq j} \quad (3.6)$$

with  $b_i$  being the transmitted power wave amplitude and  $a_j$  being the incident power wave amplitude at the  $j^{th}$ -port. The subscripted condition implies that no power waves are returned to the network from all other ports  $k$  which are considered not being stimulated but to be connected to perfect matched loads. Following the S-parameter convention  $s_{ij}$ , the first subscript ( $i$ ) always refers to the responding port or in other words to the port at which the wave is travelling outward the network. The second subscript ( $j$ ) refers to the port to which the wave is travelling towards. Assuming, power is fed into an arbitrary multiport network over the junction of port 1 and the signal is exiting the network at port 4, the determined S-parameter is the transmission coefficient  $s_{41}$ . It can be illustrated by representing the S-parameters with a signal flow graph as shown in Figure 3.2. A flow graph is representative the transmitted and reflected signals from a network. This way the S-parameters of any network can be presented.

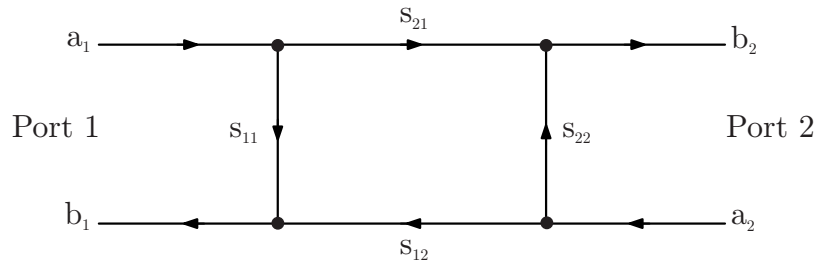


Figure 3.2: Signal flow graph representation of a 2-port network

The S-parameters are depending on the accuracy of the reference impedances (source and load) used for the measurement as well as on the frequency those are measured at and of course on the network itself including the plane of reference which defines the position where the measurements are made. Observing the characteristics of the travelling waves, the transmitted and reflected waves will be changed by the network in amplitude and phase in comparison to the incident wave, whereas the frequency remains unaffected and stays the same. Due to that fact, S-parameters are expressed as complex numbers representing magnitude and phase angle at each point of frequency. Whereas such a representation is very convenient for post-processing operations, for interpretation purposes these parameters often posed in linear form as amplitude and phase or in case of logarithmic scale with magnitude in decibels (Bode plot). In microwave theory S-parameters are often displayed on a so-called “Smith Chart” [29]. For the sake of completeness, [30] contains tables how S-parameters can be converted to and from alternative network parameters.

Typically S-parameters are provided at a set of discrete frequency points that cover the frequency spectrum of interest. Most common VNAs have a minimum frequency and do not operate at very low frequencies why S-parameters do not have DC data. These missing S-parameters data might be needed for system characterization. Therefore, special care is required to the bound beyond the lower end of the frequency spectrum and in particular to the DC component. Simulation performances can suffer at frequencies outside the frequency range given and may yields to inaccurate results up to a certain degree. Further, it may forces the simulator to terminate the solving procedure because of non-defined data in part or all of the frequency range [31]. However, software packages typically used in this context handle this issue by providing mechanism to extrapolate values for S-parameters down to DC from the known data. Overall, in literature this concern is discussed as DC extrapolation. The issue that arises in this context is how to correctly ex-

trapolate the data down to DC. Several extrapolation techniques are proposed in literature how to treat with this matter. Following [31], two popular extrapolation approaches are constant (closest known data point used) and linear (the two closest known data points used) extrapolation. Both techniques are approximations and can, if chosen incorrectly, cause severe errors and even simulation convergence issues. In [32] it is proposed to linearly extrapolate the magnitude and unwrapped phase, derived from the first 10 lowest frequency points. [33] may uses a rational polynomial to fit the data, which implicitly extrapolates the data beyond the original frequency spectrum. In [34] a DC extrapolation method is demonstrated based on sampling theorem and causality in terms of the Hilbert transform. According to [35] a S-parameters extrapolation for frequencies down to DC can be achieved by considering a S-parameter in particular on the Smith Chart. With any DC extrapolation scheme performed, one needs to be aware that there is no guarantee for physical trueness. When carrying out simulations, anomalous results can occur that may not physically possible. The phase of a network's transfer function must be zero at DC [36]. Hence, the S-parameters imaginary part would be zero at the DC point. This may no always be the result when using extrapolation techniques. One possiblity around this issue would be to manually add the DC term to the S-parameter data set (Touchstone file) [31, 37]. Even so one has to know the expected real values for DC. In this work the DC extrapolation has been considered but not used due to the risk of improper extrapolation. Unlike inverse fast Fourier transform (IFFT) processing where the DC information is critical [35] for the used modeling technique it is not an imperative. Furthermore, it is not relevant for analysis of high-frequency transients.

## 3.3 Measurement of Scattering Parameters of an N-port Network

### 3.3.1 Vector Network Analyzer

Today various simulation software packages (e.g. MATLAB or Agilent Advanced Design System (ADS)<sup>1</sup>) routinely used in the high-frequency engineering as well as finite element analysis software packages such as COMSOL Multiphysics<sup>®2</sup> permit the extraction and manipulation of network parameters such as Y, Z, and S-

<sup>1</sup><http://www.home.agilent.com/en/pc-1297113/advanced-design-system-ads>

<sup>2</sup><http://www.comsol.com/>

parameters of electrical networks in a relatively simple process. If used to characterize a circuit, they are typically measured based on experiments by the use of VNAs.

The capability to provide error corrected amplitude and phase characterization of active and passive components makes the VNA to a powerful and flexible measuring instrument and thus to one of the standard test tools for radio frequency (RF) and microwave engineers. A VNA typically measures the S-parameters because reflection and transmission of electrical networks can be measured accurately even at high frequencies. To determine the S-parameters of components, circuits, cables or antennas, the VNA sweeps a sinusoidal electrical signal linearly or logarithmically through a user specified frequency range and measures the magnitude and phase characteristics. The measurement of both, magnitude and phase is necessary for a complete characterization of the DUT. Even though the magnitude only data might be fully sufficient in many situations (e.g. gain of an amplifier), for the development of circuit models for simulations the phase information is needed as well. Furthermore, the phase data is used by the VNA itself to perform vector error correction.

As the DUT features a unique performance at a certain frequency from one port to another, the S-parameters are preferably determined within a certain frequency range of interest with a high density of frequency points, typically hundreds or sometimes exceeding one thousand. The frequency range can start as low as in the range of a few hertz and stop as high as in the gigahertz range. A complete sweep is usually just a matter of a few seconds or less and measures directly the corresponding S-matrix at each frequency point. The comprehensive and convenient measurement procedure supports the proposed approach.

Although multiport VNAs have become more popular in the recent years and commercially available, 2-port VNAs are most common since those are more reasonable in price. 2-port VNAs are often used to characterize 2-port networks such as amplifiers and filters. Modern VNAs allow exporting the set of S-parameters in the unified industry-standard format „Touchstone<sup>®</sup>“, specified in [38] which can be imported easily by computing software packages such as MATLAB and RF Toolbox. The specification gives a clear instruction how a set of S-parameters must be stored in the output file in order to facilitate an easy readout. The files are ASCII data files and are editable with any text editor.

In this work a 2-port VNA from Agilent has been used (Figure 3.3). Beside a full 2-port calibration it provides S-parameter measurements from 30 kHz to 6 GHz by

1601 frequency points in total. If the frequency resolution is not adequate for any reason, it is possible to make a second measurement (or even more) and to manually combine the data recorded. This VNA does not support the output of Touchstone files (\*.s2p). Therefore, additional steps are required to obtain the desired output file. This concern is discussed in Appendix B - B.4.



Figure 3.3: 2-port vector network analyzer (VNA) Agilent 8753ES available at the National High Magnetic Field Laboratory (NHMFL) [39, modified]

Figure 3.4 shows the principle internal setup of a conventional 2-port VNA. In addition to the internal source which provides the RF sweep output signal, the VNA includes three measurement channels denoted as R, A and B. To determine the S-parameters of a 2-port network the evaluation of reflection and transmission of traveling waves at both ports is required. For this purpose, channel A and B measures the voltage of reflected and transmitted waves in terms of magnitude and phase. The reference channel R is employed to measure the incident wave and hence serves as reference port [24, pp. 188-189].

Following this, a single S-parameter can be obtained by evaluating the ratio of either A/R ( $s_{11}$ ) or B/A ( $s_{21}$ ). The separation of incident and reflected waves at the input port of the DUT is achieved by means of a Dual-Directional Coupler [24, pp. 188-189]. Considering the measurement arrangement, to measure the S-parameter  $s_{12}$  and  $s_{22}$ , the DUT has to be reversed theoretically [24, pp. 188-189]. Fortunately, in practice most common VNA are capable to determine both, the forward and reverse S-parameters in one single measurement without manually reversing the DUT. This is done internally fully automatic by means of electronic switches.

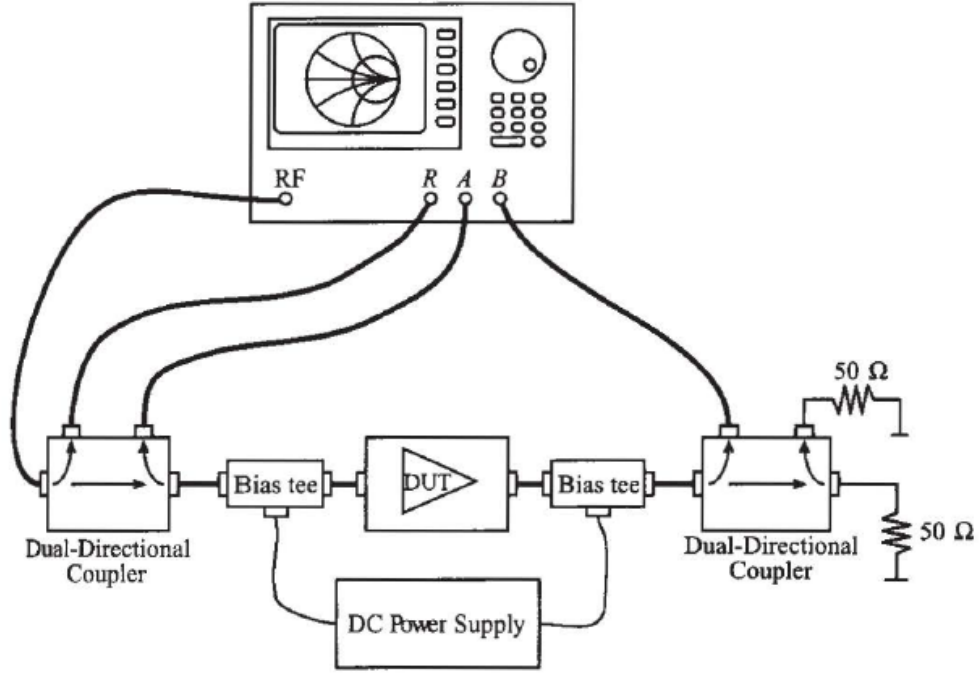


Figure 3.4: Measurement system for  $s_{11}$  and  $s_{21}$  S-parameters using a 2-port vector network analyzer (VNA) [24, p. 189]

### 3.3.2 Multiport Measurement by Means of a 2-Port Vector Network Analyzer

Common components of a 3-phase power system such as rotating machines, power electronics (DC/DC converter, DC/AC inverter) or cabling are multiport networks. This encounters the question how to characterize a multiport network ( $N > 2$ ) using a 2-port VNA. Referring to [40] several partial 2-ports measurements must be performed with the 2-port VNA connected to various combinations of the  $N$ -port network while terminating all other remaining  $(N - 2)$ -ports of the DUT with perfectly matched loads (system impedance, e.g.  $50\Omega$ ) to follow the definition of S-parameters. The number of required measurements can be found by

$$\binom{N}{2} = \frac{N(N-1)}{2} \quad (3.7)$$

where  $N$  is the number of network ports. Note, equation (3.7) implies, that forward and reverse S-parameters of the DUT are determined in one single measurement. In case of an upgrade to a newer one (e.g. 4-port VNA), it might be important to know, that for an  $M$ -port VNA where  $M$  is even and  $N$  is a multiple of  $\frac{M}{2}$ , it is

conjectured that the required number of measurements is given by

$$\frac{N(2N - M)}{M^2} \quad (3.8)$$

As shown in Figure 3.6, for a 4-port network (e.g. DC/DC converter, DC bus) for example six 2-port measurements need to be conducted. For instance, in the first 2-port measurements the VNA port 1 is connected to port 1 of the DUT and VNA port 2 connected to port 2 of the DUT. The remaining ports 3 and 4 of the DUT terminated by a  $50\Omega$  load. Then, the measurement result yields a  $2 \times 2$  partial S-matrix of the DUT containing the S-parameters  $s_{11}$ ,  $s_{12}$ ,  $s_{21}$  and  $s_{22}$ . In the second 2-port measurement, VNA port 1 is connected to DUT port 1 and VNA port 2 connected to DUT port 3. The remaining ports 2 and 4 of the DUT are again terminated by a  $50\Omega$  load. The measurement result yields again a  $2 \times 2$  partial S-matrix of the DUT containing the same S-parameters as before, but those are now equivalent to  $s_{11}$ ,  $s_{13}$ ,  $s_{31}$  and  $s_{33}$  respectively. Furthermore, it can be seen that diagonal S-parameters are measured multiple times. Generally,  $N - 1$  independent measurements of the reflection coefficient  $s_{ii}$  at each of the four ports are made.

Continuing this process with the remaining 2-port measurements in the same manner, six partial 2-port measurements will be obtained in total. Each of these  $2 \times 2$  matrices becomes a submatrix of the complete  $4 \times 4$  S-matrix describing the power waves entering or exiting the 4-port network. Following Figure 3.5, each  $2 \times 2$  submatrix can be represented by a square where each corner corresponds to the location of the four submatrices elements in the complete reconstructed  $4 \times 4$  S-matrix.

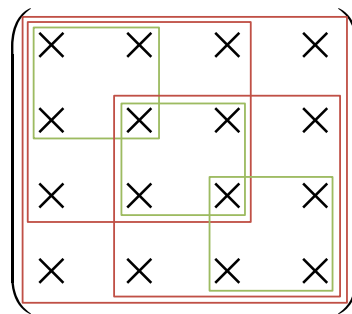


Figure 3.5:  $2 \times 2$  submatrices of a 4-port network. Each submatrix is represented by a square with corners at the locations of the four submatrix elements in the complete  $4 \times 4$  S-matrix [40, modified]

As can be seen, three (green colored) of the in total six squares are located next to

each other on the main diagonal of the complete  $4 \times 4$  S-matrix. The submatrices along the main diagonal has been used in its entirety with respect to the merging of the individual submatrices. From the remaining submatrices (red colored) only the off-diagonal coefficients located in the bottom left and upper right corner have been used respectively. This kind of segmentation can be applied to any multiport network. The assembling of the measurements is realized by a tool, described in Appendix B - B.5.

Table 3.1 shows the required measurements of many common 3-phase power system components.

N-port	2-port	3-port	4-port	5-port	6-port
Measurements	1	3	6	10	15

Table 3.1: Required measurements of a N-port network using a 2-port VNA

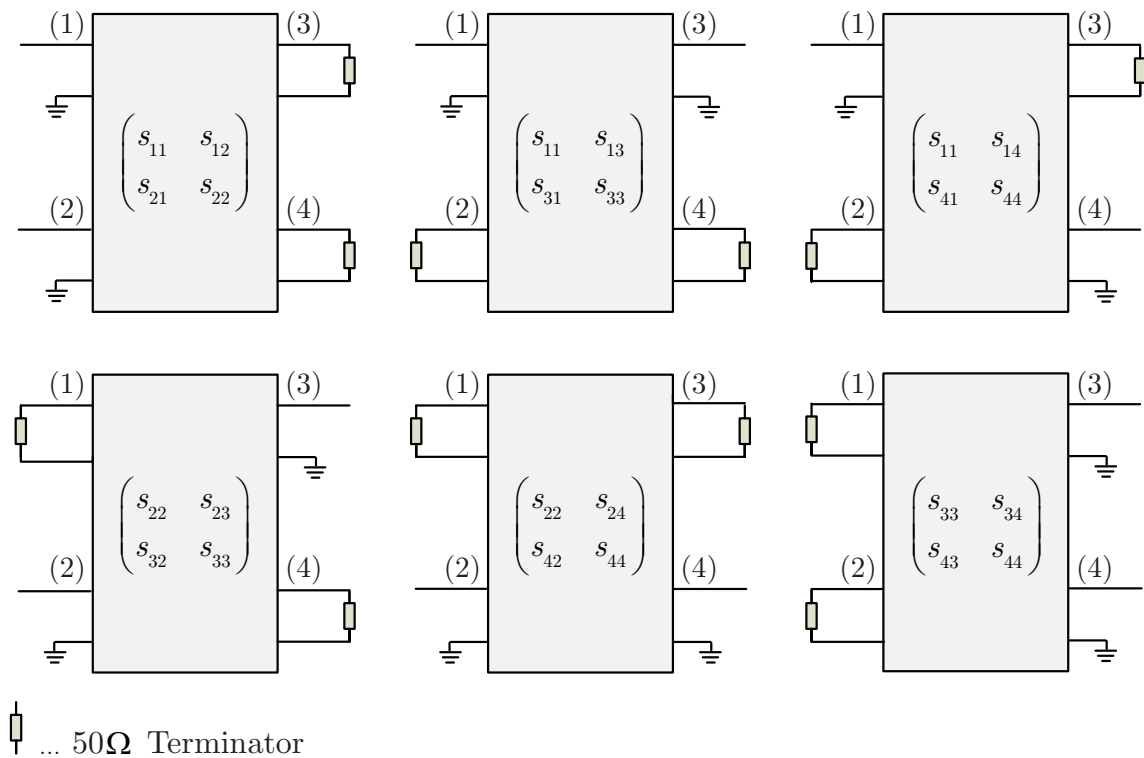


Figure 3.6: Different measurement combinations of a 4-port network using a 2-port VNA. (x) denotes the corresponding network port. The matrices contain the corresponding S-parameters obtained by each measurement respectively.

### 3.3.3 Measurement of Purdue's Small-Scale Testbed Components

Students under the supervision of Prof. Steve Pekarek at Purdue University built an experimental small-scale testbed of a simplified DC shipboard power system for grounding studies. This testbed has architectural similarities to MVDC systems being investigated for future naval ships. The power electronics include an American Power Design DC/DC converter with a switching frequency of 85 kHz with a 100 V/100 W output rating and a custom-designed 3-phase inverter with a switching frequency of 100 kHz and variable frequency output. In this work both, the S-parameters of the DC/DC converter and the 3-phase inverter have been measured.

For the measurement a typical setup including the VNA, a calibration kit as well as a set of cables and loads has been used. All components featuring an impedance of  $50\ \Omega$ . To obtain measurements with highest possible accuracy, the following steps have been considered and observed:

1. The accuracy of the measurement strongly depends on the accuracy of the VNA as well as on the port match. For this reason the VNA must be calibrated before any S-parameter measurements are performed. A good calibration is dependent on the quality of the calibration kit and the correctness and repeatability of the device connections. This requires the use of phase stable measurement leads. Accordingly to the technical features of the used 2-port VNA a full 2-port calibration was performed. Such a calibration measures the calibration data by connecting an open standard, a short standard and a load standard to the two test ports. One of the calibration issues is the elimination of the impact of the leads between the VNA and the DUT, meaning that the reference plane is shifted to the connectors of the DUT.
2. Discontinuity in the  $50\ \Omega$  environment causes unwanted scattering (reflection) of traveling waves. Therefore, connections have been made carefully not only to avoid misalignment and connector damage but also to prevent inaccurate measurements.
3. Even in use of phase-stable leads it was attempt to flex and straighten the cables as little and seldom as possible.
4. The quality of  $50\ \Omega$  termination resistors on unused ports is important.

The connection between DUT and VNA is commonly made by coaxial, phase-stable measurement leads which typically feature appropriate RF connectors (here: Type

N-connectors) at both ends. Common electrical components found in any power system regardless of whether on ship or off-shore do not provide this type of connection. Therefore, in order to perform the measurements the power electronics devices had to be prepared for RF measurements first. Figure 3.7 shows the prepared DC/DC converter and DC/AC inverter.



Figure 3.7: Power electronics of the experimental small-scale testbed used for grounding studies at Purdue University. DC/DC converter (left) and DC/AC inverter (right) after the preparation with mounted RF connectors (Type N-connectors)

As mentioned in the previous section, to obtain all 16 single-ended S-parameters a sequence of six measurements is needed. All diagonal coefficients ( $s_{11}$ ,  $s_{22}$ ,  $s_{33}$ ,  $s_{44}$ ) are measured thrice respectively. Under ideal measurement circumstances and the use of perfectly matched loads, the corresponding S-parameters associated with any of the other three ports should be identical. This cannot be met in practice since there are always unavoidable changes in the external port impedances seen by the multiport DUT caused due to the mismatch of the terminations of the unused ports. The imperfect terminations distort the S-parameters by the reflective characteristics of the terminations and actually violates the definition of the S-parameters. Naturally also the off-diagonal elements  $s_{ij}$  are error-prone up to a certain degree. However, it is known that in practice the requirement of perfectly matched loads cannot be realized with sufficient accuracy, especially with low quality terminations.

Following the measurement result in Figure 3.8, it can be seen, that the difference between a single set of diagonal S-parameters is very little in high frequency range. But below approximately 1 MHz a noticeable difference can be observed (partially at both devices). Tracking down this issue yielded to the assumption, that the difference arises from a bad termination of the VNA itself. In the course of this,

it turned out that the VNA used for the measurements has not been calibrated by the manufacturer for years. To minimize the difference the arithmetic mean of the values of each diagonal element has been taken and is discussed in Appendix B - B.5. An exact technique to solve this practical problem is known as „Scattering Parameter Renormalization Transformation“ [40].

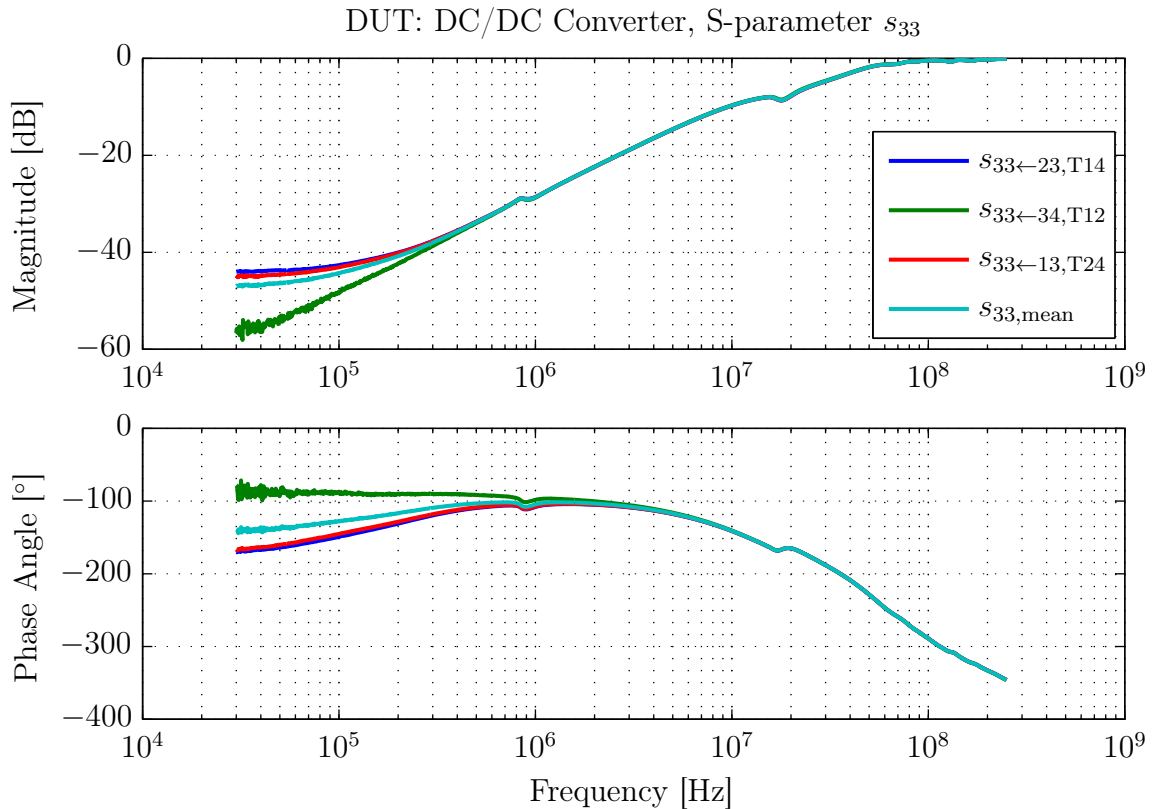


Figure 3.8: Measurements of the reflection coefficient  $s_{33}$  of the DC/DC converter with enclosure measured at 1601 frequencies ranging from 30 kHz to 250 MHz.  $s_{33\leftarrow 23,T14}$  denotes the reflection measured at port 3 when port 1 and 4 are terminated.  $s_{33\leftarrow 34,T12}$  denotes the reflection measured at port 3 when port 1 and 2 are terminated and so on.

A good measurement setup is characterized by highly reproducible results. For this reason, the DC/DC converter was measured twice once without enclosure and a second time with enclosure. It turned out that the measured results without enclosure were not reproducible. Without metallic enclosure the measurement is highly dependent on the surrounding such as electromagnetic sources. To achieve a superior shielding and hence reproducible results, it is necessary to put the DUT in a metallic enclosure. The ground potential of the DUT has been connected to ground of the VNA by contacting the enclosure and the shield of the coaxial cables (metal

body of N-connectors). Finally it should be mentioned, that the measurements have been performed with a signal excitation of the VNA of +10 dBm (maximum output power) and in non-operating conditions of the power electronic devices (i.e. no power supply). Furthermore, a logarithmic sweep was used.

Figure 3.9 shows the measurement of the transmission coefficient  $s_{34}$  of the DC/DC converter. Whereas the difference in this context low frequency range is acceptable, with increasing frequency the impact is considerable. However, this transmission coefficient allows the interpretation of traveling waves moving towards port 4 to port 3. To continue the interpretation with regard to voltage transients in case of a single rail-to-ground fault, it can be seen, that voltage transients within a frequency range of 30 kHz up to approximately 10 MHz would propagate through the device with virtually no attenuation. Higher frequency transient overvoltages would experience an attenuation up to  $-20$  dB at port 3.

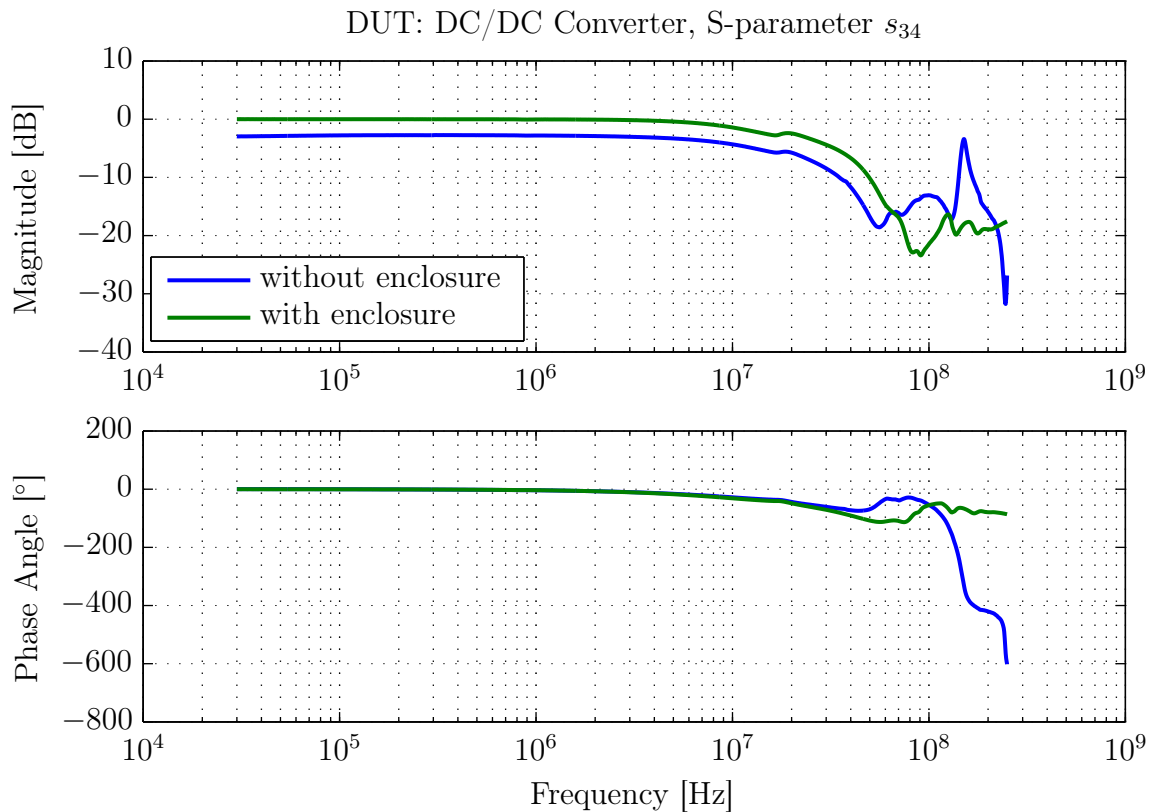


Figure 3.9: Measured transmission coefficient  $s_{34}$  of the DC/DC converter with and without enclosure. Measured over the frequency range from 30 kHz to 250 MHz at 1601 frequencies.

## 3.4 Model Implementation and Validation

### 3.4.1 Model Implementation

The implementation of a circuit level model from S-parameter measurements is accomplished in the MATLAB/Simulink [41] graphical programming environment with SimPowerSystems. The initial choice using this software package is based on the availability and experience as well as on the fact, that this computing platform together with the simulation tool PSCAD/EMTDC is commonly used in ESRDC activities for shipboard power systems simulations.

The basic implementation consists of three distinct steps:

1. Fitting a (modified) rational function to the frequency domain S-parameters data
2. Compute the transfer function and build the rational model blocks for each S-parameter
3. Incorporating these blocks into a circuit level model

#### 3.4.1.1 Rational Function Fitting

In the previous chapter it has been described how to obtain S-parameters of an N-port network. The result is a rather extensive set of recorded 50  $\Omega$  S-parameters which is stored in an sNp (N-port) Touchstone data file. In order to use these data for simulation purposes, the complex frequency domain data have to be fitted.

In the previous chapter the lowercase “s” is used for S-parameters which might confuse since in the Laplace domain the same character represents the complex frequency. For this reason in this section S-parameters are indicated with an uppercase “S”.

Referring to [37, 42, 36, 43] the objective of the fitting procedure (“rational fit”) is to create a mathematical model from the complex frequency domain data. Conceptually, this model would be a ratio of polynomial in the Laplace domain  $s$ . Following this, a finite set of measured data (e.g. a single S-parameter) can be approximated by

$$S_{12}(s) = \frac{a_N s^N + a_{N-1} s^{N-1} + \dots + a_1 s + a_0}{b_M s^M + b_{M-1} s^{M-1} + \dots + b_1 s + b_0} \quad (3.9)$$

where  $s = \sigma + j\omega$  is the complex frequency with  $\omega = 2\pi f$ .

The polynomials involved with this approximation are typically of a high order (e.g.  $M > 30$ ) and high frequencies are involved as well. When modeling high speed serial data physical interconnects, the upper bounds of frequency are often well over 10 GHz. This creates a serious numerical challenge for the above formulation. The solution is to reformulate the problem into a more numerically friendly canonic form, a partial fraction expansion

$$S_{12}(s) = \sum_{m=1}^M \frac{c_m}{s - p_m} + d \quad (3.10)$$

where  $p_m$  are pole locations,  $c_m$  are the residues to the corresponding poles and  $d$  is the direct feedthrough term which appears if  $M = N$ .

This approximation works well for lumped element systems which naturally have a finite order. But the measurements have been made on distributed systems which in principle, have an infinite order. The distributed nature is due to the measurements being made on physically large elements that behave like transmission lines. One manifestation of this behavior is a time delay for end-to-end off-diagonal (transmission) measurements such as  $S_{12}$  and  $S_{21}$  referring to a 2-port network. A small modification can be made to the partial fraction expansion to include the time delay, a so-termed modified rational function

$$S_{12}(s) = \left( \sum_{m=1}^M \frac{c_m}{s - p_m} + d \right) e^{-s\tau} \quad (3.11)$$

where  $\tau$  is a coarse estimate of the time delay.

Including this delay term can significantly reduce the order ( $M$ ) required to achieve an accurate model. Furthermore, the model runs faster without comprising accuracy. The parameters of the fitting routine are fairly straightforward and for the most part, the user simply sets the desired fitting tolerance and what percentage of the calculated delay (obtained from the phase curve of the measured data) is to be accounted for in the delay parameter. One can also stipulate the number of poles (and zeros) to be used, but it is typically simpler to specify a desired tolerance and let the fitting algorithm determine the required order of the system. In order to verify the accuracy of the model one must evaluate the magnitude and phase response of the model from DC ( $s = 0$ ) through the frequency range of the measurement data and beyond and compare this to the measurement data. Figure 3.10 shows the results for a 210 pole model without the delay term (Eq. 3.10) along with a 48 pole

model with the delay term (Eq. 3.11).

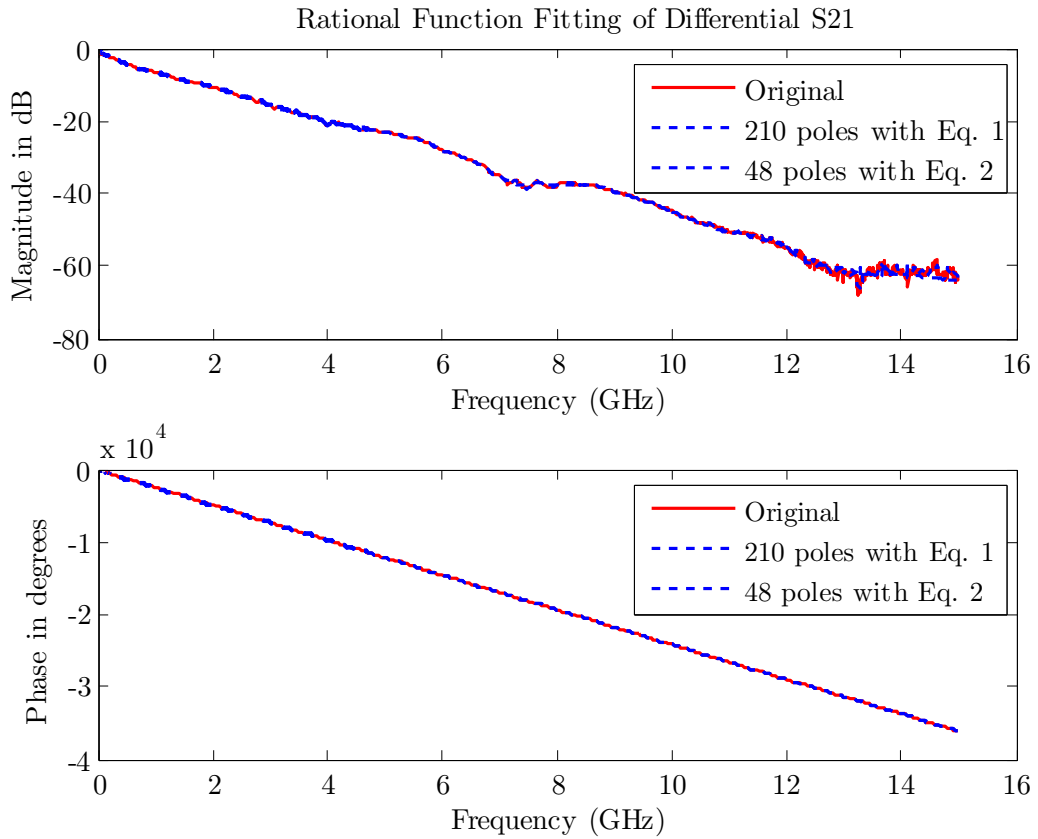


Figure 3.10: Comparison between the frequency response of the rational function object and that of the original data with equations (3.10) and (3.11) [42, modified]

The fitting technique forces the phase to be zero at  $s = 0$  and can be adapted to assume a roll-off at the high frequency end. This minimizes issues that IFFT and related techniques have had at the frequency extremes [37]. According to [44, 36], the modified rational function fitting has the following advantages compared to traditional techniques, such as IFFT:

- It provides the same level of accuracy as the IFFT method, with a model that is one or two orders of magnitude simpler
- Model order reduction can be used to trade off complexity and accuracy through the use of fitting parameters
- Typical VNA data has a low frequency cut-off why an extrapolation to DC is needed. Rational function models represent a physical transmission line and inherently constrain the phase to be zero on extrapolation to DC. Standard

IFFT techniques do not provide anything to prevent the extrapolated phase from being non-zero (corresponds to a non-physical delay). IFFT models require elaborate constraint algorithms in order to force the extrapolated phase to zero at DC.

The presented technique relies on vector fitting. References [43, 42, 36] cover the underlying fitting algorithm in more detail.

### 3.4.1.2 Generation of Transfer Function Blocks

Once the poles, residues, order and time delay are verified, a Simulink model that implements the modified rational function (Eq. 3.11) can be created. Since the system being modeled is a real physical system, the input and output are naturally real numbers. The poles therefore naturally occur in complex conjugate pairs [37]. These pairs can be combined into second order transfer function blocks. Non-complex real poles on the negative real axis of the s-plane can be included as single pole transfer function blocks. A typical rational model in Simulink is as follows:

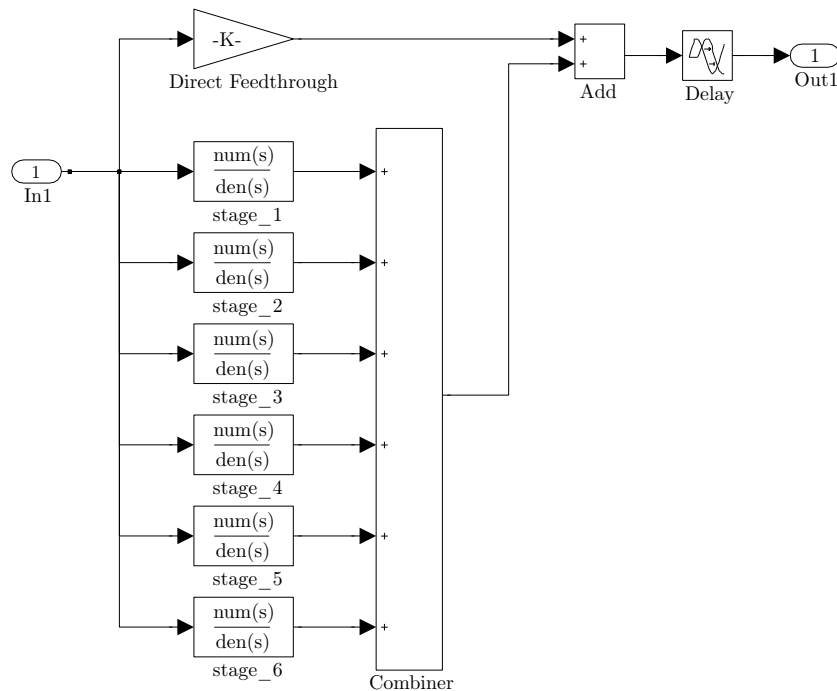


Figure 3.11: Simulink model of a rational function object representing a single S-parameter

As described, the transfer function blocks (“stages” in Figure 3.11) are of second and first order. They implement the complex conjugate pole pairs, and real poles and

the corresponding residues respectively. Note, each transfer function block always has real coefficients. This is why the poles and corresponding residues of the rational function object of each S-parameter needs to be converted into real numerators and denominators for use in the Laplace transform transfer function blocks. This is accomplished by the equations 3.12 and 3.13.

$$F(s) = \frac{c_m}{s - p_m} \quad (3.12)$$

$$F(s) = \frac{2\text{Re}(c_m)s - 2(\text{Re}(c_m)\text{Re}(p_m) + \text{Im}(c_m)\text{Im}(p_m))}{s^2 - 2\text{Re}(p_m)s + \text{Re}(p_m)^2 + \text{Im}(p_m)^2} \quad (3.13)$$

The delay time of the (transport) delay block is set by the „Delay“ of the rational function object. If set to zero the transport delay block is automatically set to support direct feedthrough. The output is controlled directly by the value of the input. This may cause an algebraic loop (see section 3.6). The gain value of the gain block is set by the direct feed term „D“ of the rational function object. However, Figure 3.11 shows a relatively low order model as compared to what real-world measurement data requires. But even this low order model would be very tedious and error prone to create manually. Fortunately MATLAB allows to automatically build and modify a Simulink model purely from MATLAB code without using the Simulink user interface. This can be achieved using MATLAB-Simulink API (application program interface) commands. This enables the option to make the construction of far more complex (higher order) models effortless.

### 3.4.1.3 Circuit Level Model Implementation

The discussion is continued on a 2-port example, but the proposed approach can be easily extended to N ports, which allows to study many of the most common components of a 3-phase power system (e.g. N = 6). The final step in the modeling process is to include the 4 rational transfer function blocks in a circuit level environment. Table 3.2 shows the number of such function blocks needed to implement a N-port network. SimPowerSystems, a toolbox for Simulink, allows to model power systems in a similar fashion as SPICE<sup>3</sup>. Unlike SPICE, it is optimized for the needs of a power systems engineer. However, the stock tool does not have the ability to model from S-parameters, but it can be extended to do so by using controlled sources and measurements of both voltage and current. From a “top level”, the S-parameter model looks as shown in Figure 3.12.

---

<sup>3</sup>Simulation Program with Integrated Circuit Emphasis [45]

N-port	2-port	3-port	4-port	5-port	6-port
Rational transfer function blocks	4	9	16	25	36

Table 3.2: Number of rational transfer function blocks needed to implement a N-port network into a time domain circuit simulation

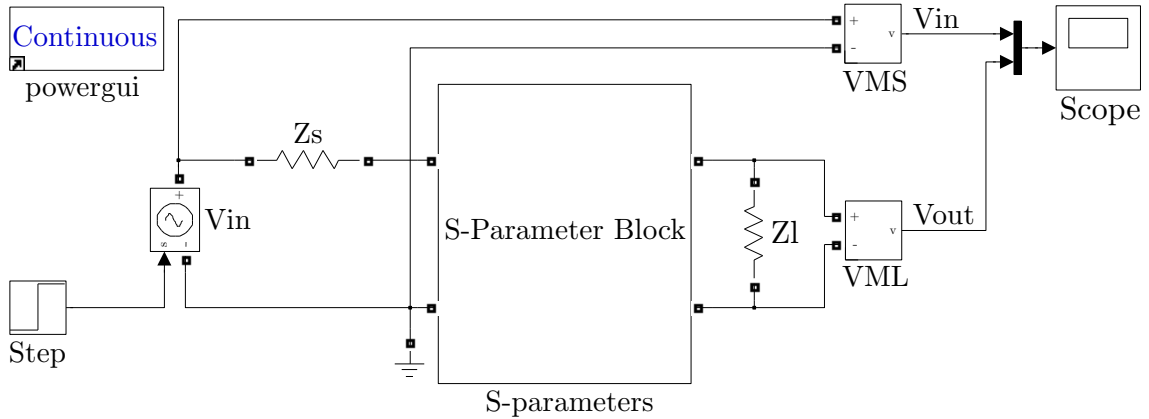


Figure 3.12: S-parameter model block built in Simulink/SimPowerSystems. Any complex passive and active sources and loads can be incorporated around the S-parameters model block

The interface between the unidirectional signal domain of Simulink and the circuit domain of SimPowerSystems is accomplished with the “Vin” block (a controlled voltage source) and the “VML” block measuring the voltage across the load „Zl“ and producing a signal labeled „Vout“. More complex passive and active sources and loads could be incorporated around the S-parameter model block. The internals of the S-parameter block are shown in Figure 3.13.

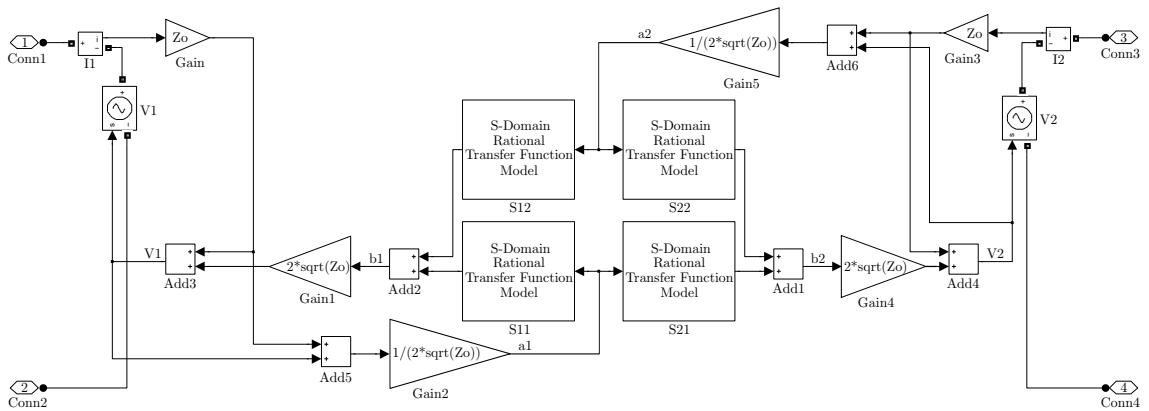


Figure 3.13: Internals of the 2-port S-parameters model block which implements the equations that link the four S-parameters to the input and output port voltage and current.

The four blocks in the central portion of the subsystem are the rational fit transfer function elements. Note that they are pure Simulink blocks with a unidirectional signal flow as indicated by the arrows. By using controlled voltage sources „V1“ and „V2“ in conjunction with current measurement blocks „I1“ and „I2“, the equations that link the four S-parameters to the input and output port voltage and current can be solved. Note that „I2“ enters port 2. The model is based on the equations 3.2, 3.3 and 3.4. The latter is a conversion to  $V_i$ . The software version of MATLAB/Simulink used for all examples in this report is 7.9.1/7.4.1 (MATLAB R2009b SP1).

### 3.4.2 Model Validation

Model validation is a necessary process to determine the degree to which the model is an accurate representation of the physical (real world) situation. The validation of the implementation described in the previous section has been conducted using the RF simulation package Agilent Advanced Design System (ADS Version 2011.10 [46]). The initial choice using this software package is based on the fact, that it is routinely used in the high-frequency and microwave electronics for circuit design. Hence, ADS allows to easily extract S-parameters from such circuits and to write the set of data into the Touchstone file format. Equally important, it allows to implement S-parameters based on Touchstone files by means of S-parameter blocks available in the component library (Data items). Furthermore, this software product is available at the Florida State University (FSU).

As can be seen in Figure 3.14, a linear time-invariant network has been defined by a circuit using passive lumped elements. The output of certain input excitation (step function) was recorded. Recording the step response is reasonable since the step function a) may be considered as system fault initiation and b) enables the evaluation over a wide range of the frequency spectrum in which voltage transients may be present. The circuit built consists of two single PI line models representing two single-phase transmission lines. A PI line model for a short section of transmission line is composed of a capacitor  $C$  shunting the signal to ground, followed by a series inductance  $L$  and resistance  $R$ , followed by another capacitor  $C$  shunting to ground. The resistor in series with the inductance describes the power loss. The two PI-segments are cross-coupled by two capacitors ( $C_5$ ,  $C_6$ ) which leads to a 4-port network configuration. The values used for the simulation are listed in Table 3.3.

Subsequently the extracted set of S-parameters, has been used to implement the network in Simulink/SimPowerSystems based on the S-parameter implementation

approach proposed. For comparison purposes the same S-parameters has been implemented in ADS using the 4-port block natively available.

Note: The S-parameter block implemented in Simulink/SimPowerSystems exhibits a controlled voltage source at input (1). This causes in this circuit configuration a parallel circuit of two voltage sources which is not allowed for technical reasons. Thus, a low-impedance resistor  $R_1$  is interconnected.

Name	$V_S$	$R_1$	$R_2, R_3$	$L_1, L_2$	$C_1 - C_4$	$C_5, C_6$	$R_4 - R_6$	$R_{on}$ (Switch)
Value	1	1	42	2.33	6	2	50	100
Unit	V	m $\Omega$	m $\Omega$	$\mu$ H	nF	nF	$\Omega$	m $\Omega$

Table 3.3: Simulation parameters used for validation

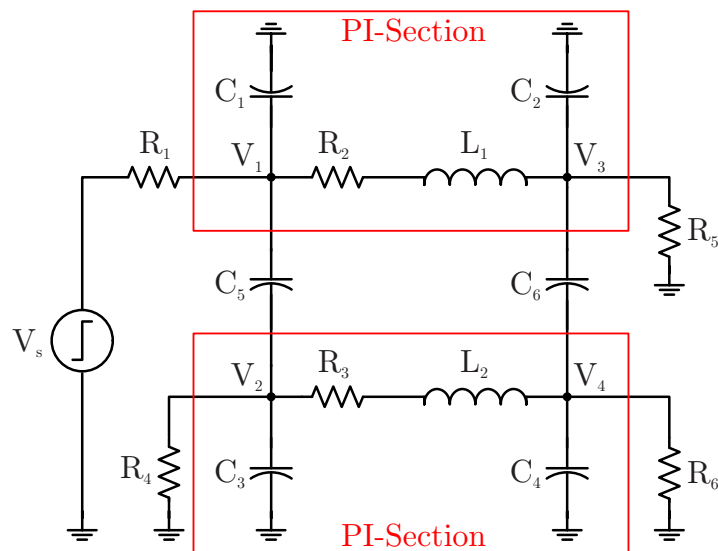


Figure 3.14: Validation circuit designed in ADS consisting of two PI-sections representing two single-phase transmission lines. Those are cross-coupled by two capacitors which leads to a 4-port network configuration.

Figure 3.15 shows an overlay of the simulation results. As can be seen the output voltages of the S-parameter model in Simulink/SimPowerSystems agree perfectly to the output voltages of the lumped element model as well as to the model based on the S-parameter data of the Touchstone file. The latter both implemented in ADS. The Touchstone file generated includes the S-parameters data from 1 Hz to 250 MHz. In order to correctly simulate a step response, the DC point is needed. This is why ADS performs an extrapolation down to 0 Hz which is never exact. The

„ringing“ at approximately  $4\ \mu\text{s}$  in the ADS simulation using S-parameter data is a result of truncating the frequency response and ADS impulse response calculations [47]. Compared to Simulink/SimPowerSystems it seems that ADS has more trouble with the lack of the low frequency data.

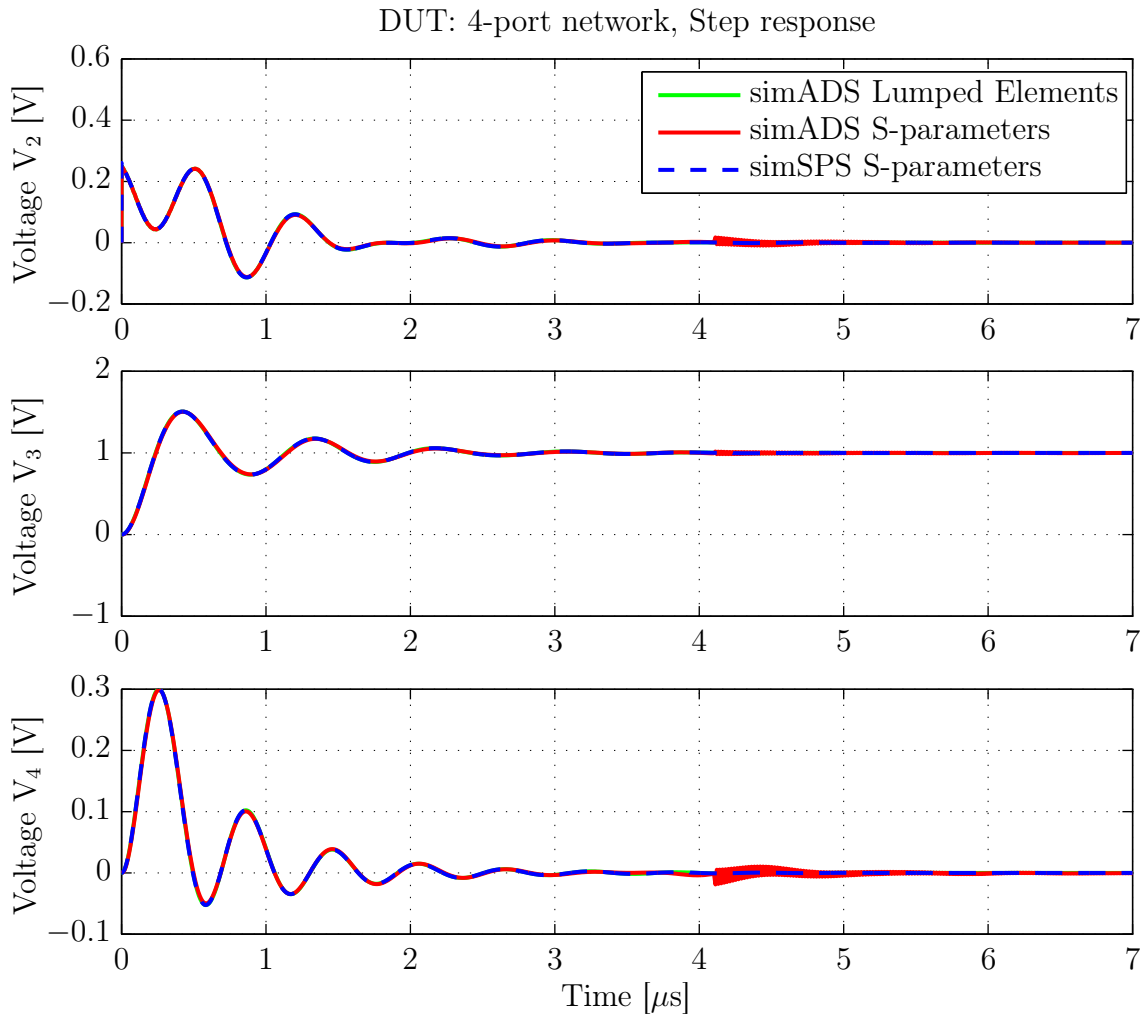


Figure 3.15: Step response of the 4-port network used for the validation process

However, following the result the accuracy of the S-parameter implementation seems to be perfectly sufficient for high-fidelity power systems simulations.

## 3.5 Circuit Simulations

### 3.5.1 Transmission Line Model (3-PI-Section)

After the validation process the next step was to implement an arbitrary cable model and integrate it in a time domain simulation. For this purpose a circuit has been built as shown in Figure 3.17. Two DC voltage sources represent the rail voltages ( $V_p$ ,  $V_n$ ) of a bipolar DC distribution bus. The midpoint of the voltage sources  $V_{dc}$  is grounded by a capacitor which represents the total capacitive coupling to ground of the DC side of a DC shipboard power system. A load is represented by resistor  $R_L$ .

First the S-parameter block has been replaced by a single-phase transmission line model based on lumped elements. As shown in Figure 3.16, the model being used consists of three cascaded single PI-sections in series which leads to a 3-segment PI model. In [20] a identical model has been used for validation purposes of a 5 kV XLPE power cable. That study provided reasonable values of all elements.

Subsequently, a transmission line model was developed in ADS and the S-parameters extracted from 1 Hz to 250 MHz. The model was implemented by means of a 2-port S-parameter block in Simulink/SimPowerSystems. Each of the S-parameter blocks features a voltage source at its input as well a voltage source at its output. The input voltage sources would be in parallel with the supply sources respectively. In order to prevent numerical instability, low-resistance resistors  $R_1$  and  $R_2$  are inserted. Also the lumped elements model features a capacitance on the input and should not directly connected to an ideal voltage source (a source with no internal resistance). Hence, a low-impedance resistor  $R_s$  is connected in series to it.

A prospective single rail-to-ground fault is initiated by a non-ideal switch (internal resistance  $R_{on} > 0.001\Omega$  in on-state) triggered by a timer. Then the negative rail voltage ( $V_n$ ) assumes ground potential. The rail voltages of the DC bus of both simulations have been recorded respectively and finally compared. As can be seen in Figure 3.18, the simulation results show a perfect agreement. The oscillation frequency is around 103 kHz.

Name	$V_{dc}$	$R_1, R_2, R_s$	$C_n$	$R_L$	$R_{on}$ (Switch)	$R$	$L$	$C$
Value	100	1	1	100	100	14	777	4
Unit	V	m $\Omega$	$\mu$ F	$\Omega$	m $\Omega$	m $\Omega$	nH	nF

Table 3.4: Simulation parameters used for the transmission line model simulation

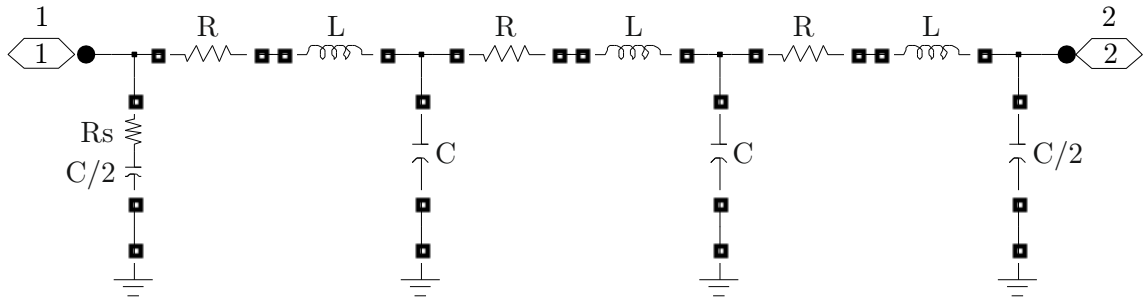


Figure 3.16: Transmission line model (3-PI-segment line model) of a monopolar DC distribution bus using lumped elements only

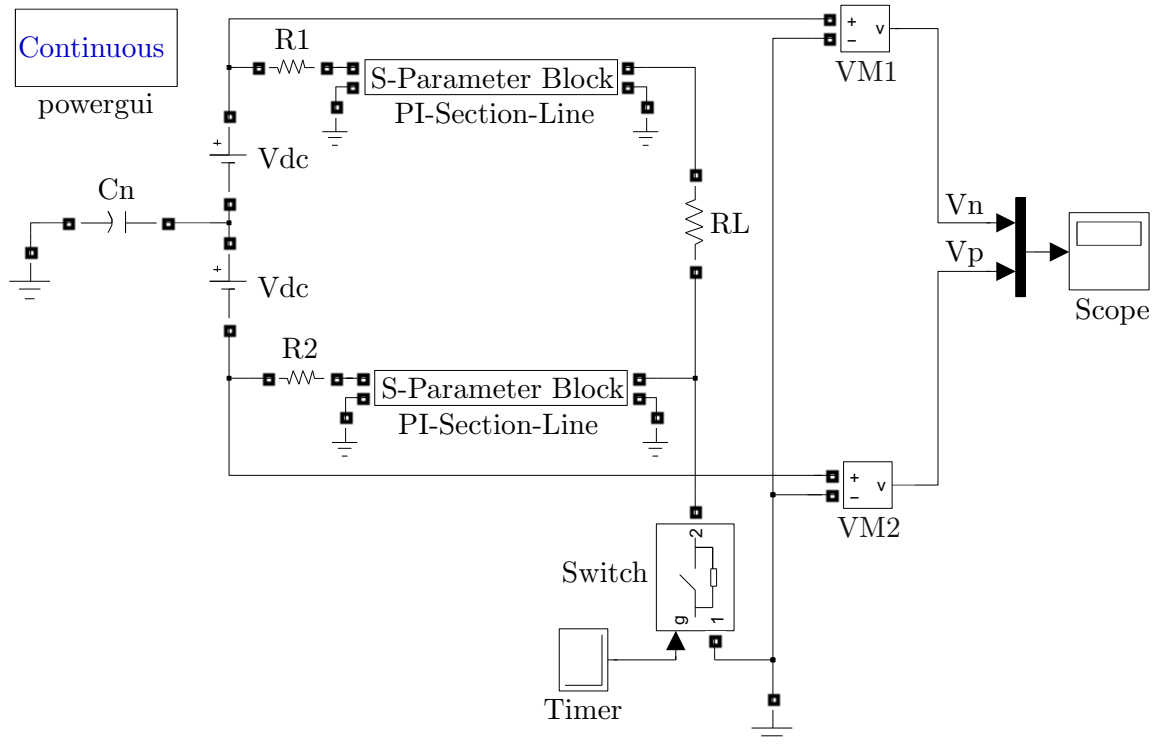


Figure 3.17: Simulation model of a capacitively grounded bipolar DC distribution bus in Simulink/SimPowerSystems with integrated 2-port S-parameter blocks

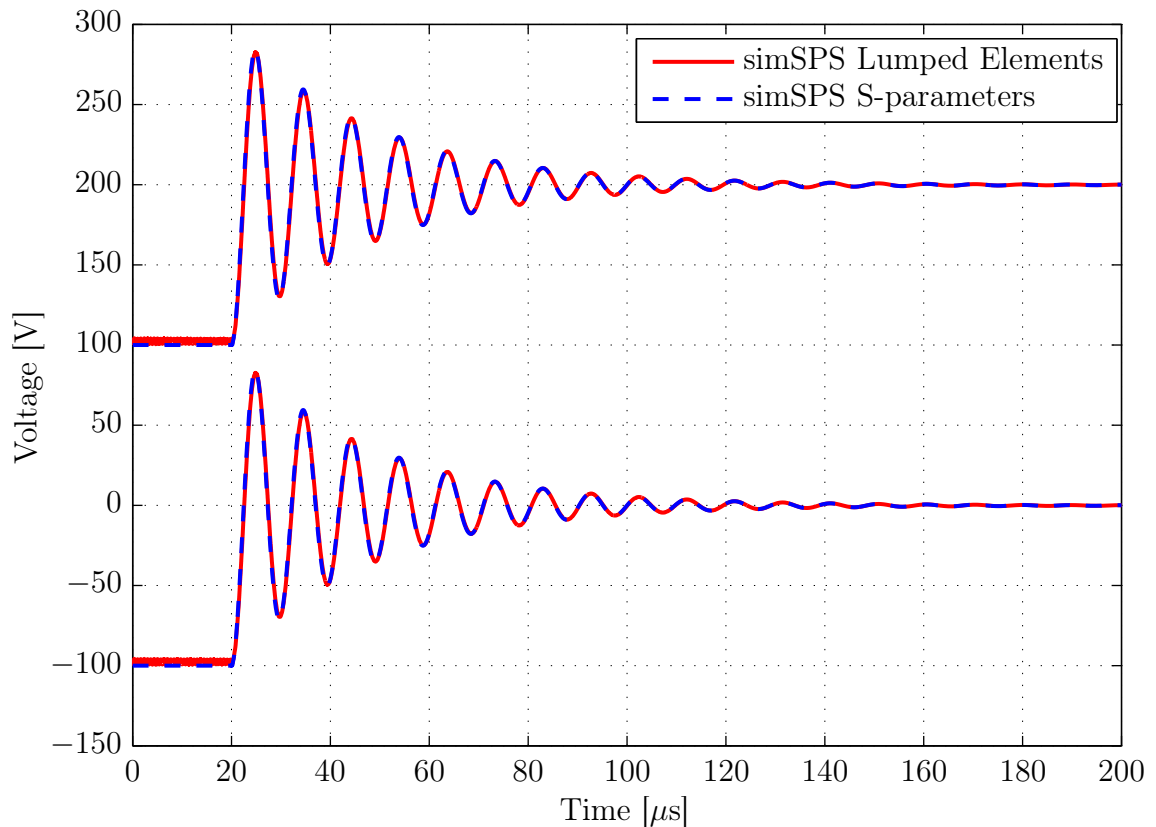


Figure 3.18: Transmission line model: Rail voltages ( $V_p$  (above),  $V_n$  (below)) of the DC bus in case of a single rail-to-ground fault at  $20 \mu\text{s}$

### 3.5.2 DC/DC Converter Model

Next the DC/DC converter was incorporated into a simple time domain simulation by its S-parameters measured (from 1 Hz to 250 MHz). The DC/DC converter represented by the S-parameters block (4-port) is fed by two DC voltage sources connected in series representative the rail voltages ( $V_p$ ,  $V_n$ ) of a bipolar DC distribution bus. The midpoint is grounded by a capacitor which represents the total capacitive coupling to ground of a shipboard DC bus. The circuit model of the S-parameter block features two voltage sources at its input as well as two voltage sources at its output. The input voltage sources would be in parallel with the ideal supply sources  $V_{dc}$  respectively (sources with no internal resistance). In order to prevent numerical instability, low-resistance resistors  $R_1$  and  $R_2$  are inserted. A load is represented by resistor  $R_L$ . The values used for the simulation are listed in Table 3.5.

Name	$V_{dc}$	$R_1, R_2$	$C_n$	$R_L$	$R_{on}$ (Switch)
Value	16.8	1	1	100	100
Unit	V	m $\Omega$	$\mu F$	$\Omega$	m $\Omega$

Table 3.5: Simulation parameters used for the DC/DC converter model simulation

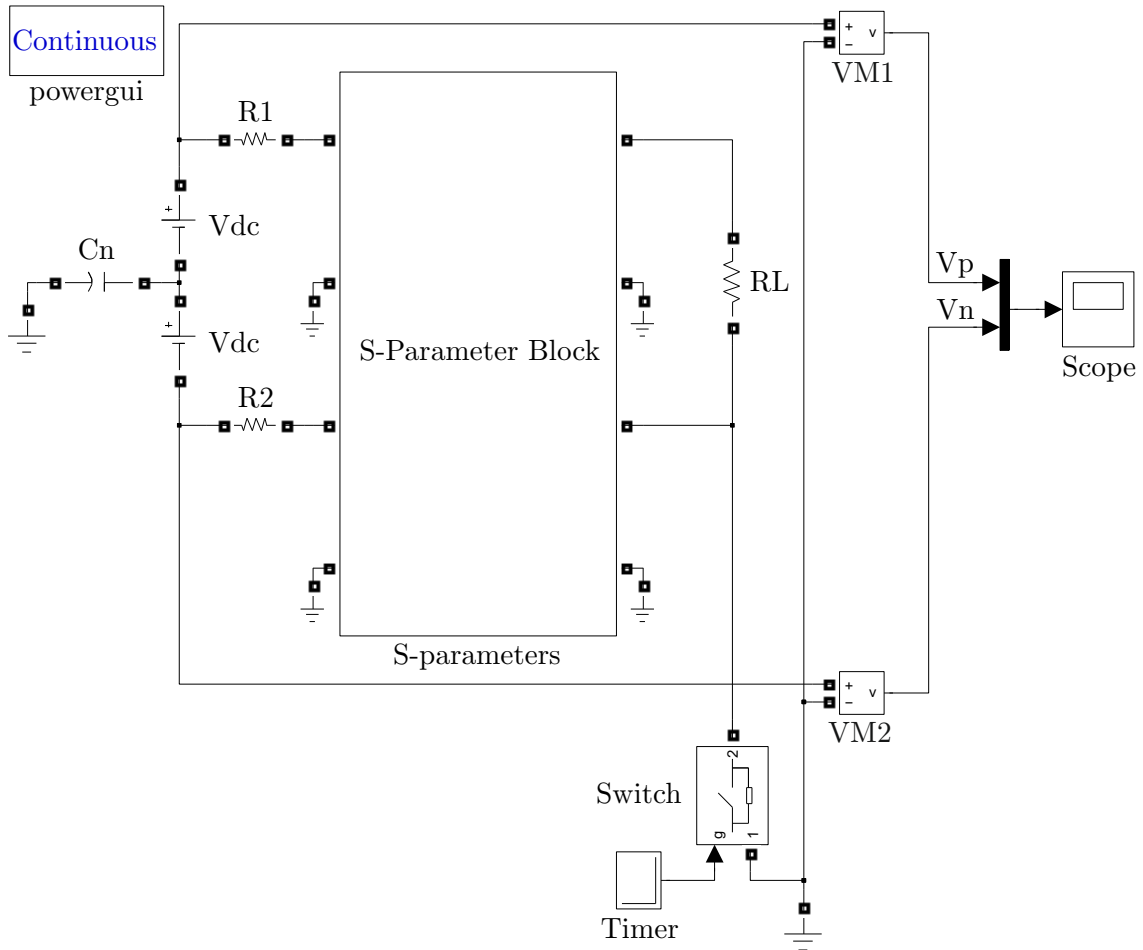


Figure 3.19: Simplified capacitively grounded bipolar DC distribution bus including a 4-port S-parameter block representing the DC/DC converter measured implemented in Simulink/SimPowerSystems

A single rail-to-ground fault is initiated by a non-ideal switch (internal resistance  $R_{on} > 0.001\Omega$  in on-state) triggered by a timer. Then the negative rail voltage ( $V_n$ ) assumes ground potential. As shown in Figure 3.20 this manifests in a high frequency oscillation on both rails. The oscillation frequency is approximately 33 MHz. Additionally the simulation features a voltage drift of both conductors of  $3.5V/\mu s$  whose cause is not clear yet. At first appearance the continuous increase of the rail voltages seems to be an ongoing charging event of the capacitor located at the midpoint

due to the particular circuit configuration. If this would be the reason, the voltage levels could exceed the input voltage. Further investigations led to the assumption that the significant voltage drift is a result of corrupt S-parameters. By the time of completion of this report, the DC/DC converter has been measured another time by means of a different VNA. Using this new set of S-parameters has shown, that the drift is significantly lower. By date, this result is not available for comparison.

This issue needs further investigations to completely understand the cause and mitigate its effects.

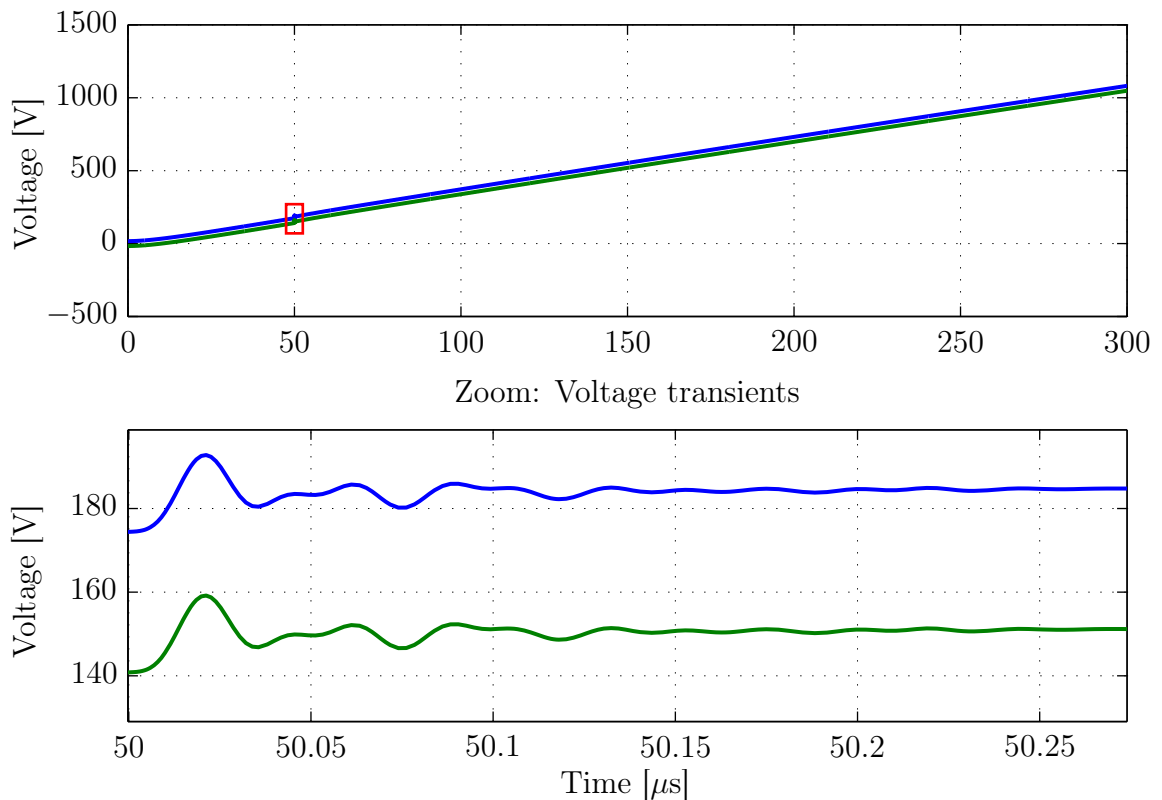


Figure 3.20: DC/DC converter model: Rail voltages ( $V_p$  (blue),  $V_n$  (green)) of the DC bus in case of a single rail-to-ground fault at  $50 \mu\text{s}$

### 3.6 Solver Settings and Pitfalls

The underlying computational engine of MATLAB/Simulink is a variable-step Ordinary Differential Equation (ODE) solver. The implementation technique proposed here makes use of the add-on tool SimPowerSystems to do the circuit level work needed and further to achieve SPICE-like behavior in a Simulink model. To solve

the model the SimPowerSystems technology maps the circuit level description into a state space format that can be simulated with an ODE solver. This can often lead to so-called “algebraic loops” [37]. In the simplest case an algebraic loop is present in a Simulink model if the output of a particular block (e.g. the summation block „sum“) is directly fed to at least one of the inputs. This results mathematically in an algebraic loop which is difficult to solve numerically. Fortunately the Simulink engine has been optimized over many years to efficiently handle this computational challenge [37].

The simulations performed have shown that the accuracy of the numerical simulation results as well as the simulation speed can strongly depend on solver settings. Improper solver settings such as type, step sizes, tolerances or solver reset method can significantly slow down the simulation and lead to inaccurate results. In worst case it can lead to algebraic loop(s) that cannot be solved by MATLAB/Simulink. Pushing the solver options to suitable settings for efficient performance is not always readily achievable since this requires advanced skills and experience. An overview and guidance which solver types are available, how to select a solver and how to specify solver options for efficient, customized execution can be found in the documentation center of MATLAB [48, Choose a Solver, Solver Pane, Customizing Solvers for Physical Models, etc.]. Sometimes it requires several trials before suitable settings are found.

It has been found that the ode23tb and ode15s variable-step stiff solvers are more robust than fixed-step solvers and more suitable for simulation models including S-parameter blocks. Those solvers are typically used for power systems simulations [49]. Stiff differential equations are used to solve the problem. But there is no exact definition of stiffness for equations why numerical methods of the solver types behave different and may become unstable in some cases. However, following the recommendation of MATLAB, the ode23tb stiff solver with relative tolerance set to 1e-4 is recommended in order to achieve best accuracy and simulation performance. The relative tolerance has to be small enough to achieve numerical stability. For some highly nonlinear models it may be necessary to set the "Solver reset method" parameter to "Robust". In addition to these settings, it was necessary to find reasonable values for the remaining settings such as step sizes, tolerances as well as the algorithm settings.

Table 3.6 shows the solver settings found to work very well for the simulations performed in MATLAB 2009b SP1 and may serve as starting point for future optimizations. With respect to the simulation times used for the different simulations

(7 - 300 $\mu$ s) and the corresponding solver settings chosen, the actual simulation time (real time) takes just a few seconds on a reasonably equipped computer respectively. Note, these settings may need to be adjusted on case by case basis depending on the characteristics of the simulation model and the version of MATLAB.

<b>Simulation</b>	<b>N-port Validation</b>	<b>Transmission Line Model DC/DC Converter</b>
Type	Variable-Step	Variable-Step
Solver	ode23tb (stiff/TR-BDF2)	ode15s (stiff/NDF)
Initial Step Size	auto	1e-11
Min Step Size	auto	auto
Max Step Size	1e-9	1e-7
Relative Tolerance	1e-3	1e-4
Absolute Tolerance	auto	1e-4
Solver Reset Method	Robust	Fast
Algorithm	Nonadaptive	Nonadaptive

Table 3.6: Solver settings used for the simulations performed in Simulink/SimPowerSystems. All other settings than those stated here were left at default values (default settings depend on solver type)

## 4 Conclusion

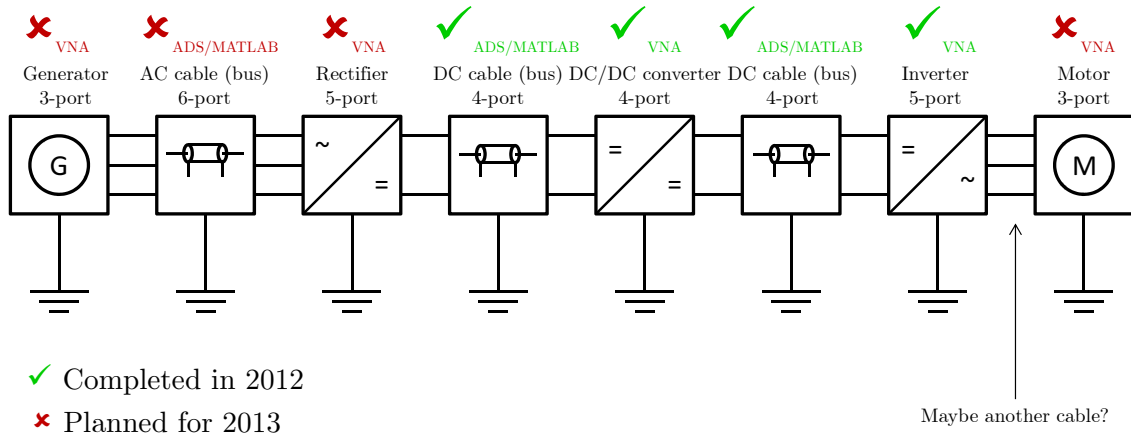
One subtask within the Electric Ship Research and Development Consortium (ES-RDC) effort focuses on grounding aspects of direct current (DC) systems operated at medium voltage (MVDC). One of the research thrusts is the transient behavior of the DC bus as a function of the location of a prospective single rail-to-ground fault. For higher accuracy, specific models of the system components might be required, which are tailored to grounding studies in shipboard power systems. One part of ongoing research at the Center for Advanced Power Systems (CAPS) evaluates the modeling and characterization approach of common components of a 3-phase shipboard power system based on the concept of S-parameters. This work provides the essentials to perform further investigations on this subject in the future.

In this work S-parameter models have been introduced for transient power systems modeling. A method has been proposed how to incorporate S-parameters in power systems software packages. A S-parameter block has been built which allows to study common components of a shipboard power system. Validation based on step response has been conducted using Agilent Advanced Design System (ADS). It has been shown that the technique proposed here is accurate, valuable and feasible for high-fidelity power system simulations. It has been found that the choice of solver settings are critical. In future it might be reasonable to focus on the cause more detailed in order to possibly figure out whether there are certain indicators which play a part in contributing to the finding of proper solver settings. The emphasis of S-parameters implementation is on Simulink/SimPowerSystems. Following this, it may should be proven if it is reasonable and possible to add the built N-port S-parameter blocks to the component library of Simulink. Moreover it is assumed that the implementation method is suitable for the software package PSCAD/EMTDC as well. Investigation has shown that this simulation tool supports the integration of  $N^{\text{th}}$  – order Laplace domain transfer functions. Based on this knowledge it needs to be vetted if this tool provides the opportunity such as MATLAB to automatically integrate a simulation model into a time domain simulation on the basis of code execution.

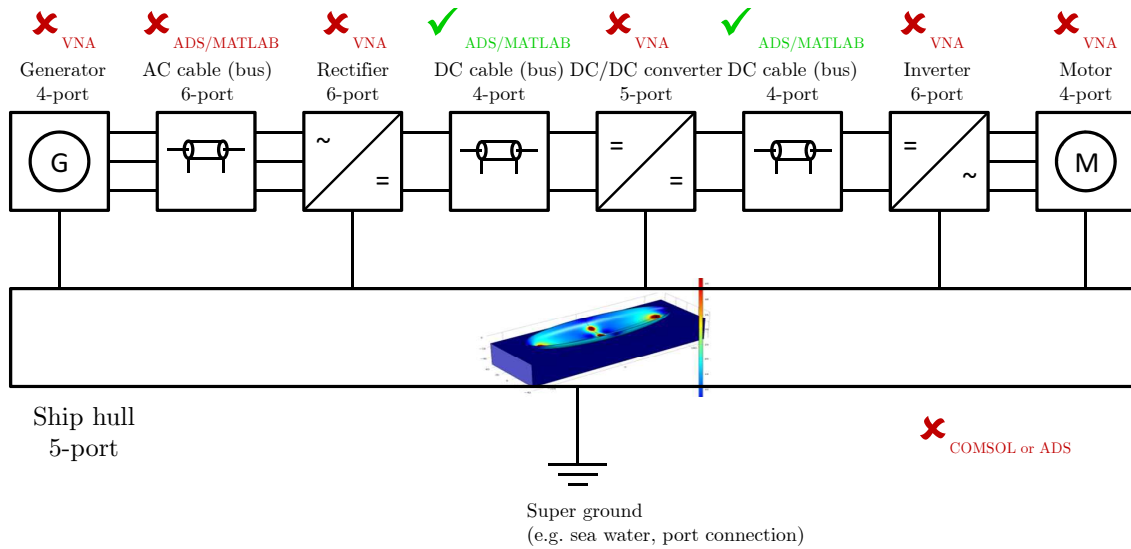
A complete S-parameters characterization of power electronics components of a grounding testbed by Purdue University has been conducted by means of a 2-port vector network analyzer (VNA). The measurements were carried out in collaboration with the National High Magnetic Field Laboratory (NHMFL). It has been shown how to measure multiport networks with a 2-port VNA. The VNA available does not support the output of Touchstone files (\*.s2p). MATLAB tools have been created which enable to handle the extensive amount of files obtained by 2-port measurements as effortless as possible. Further, a tool has been established which allows to study and visualize complex frequency domain data of network parameters less time-consuming. Likewise, a tool has been created to obtain the S-parameters rational function objects on the basis of vector fitting. The fitting approach is needed to implement a Device-Under-Test (DUT) based on its S-parameters into a time domain simulation. The modeling technique presented seems to be an effective solution for the representation of multiport networks. The conclusion were supported by simulation and results from preliminary experiments.

The next step will be to validate the S-parameters-based model by time domain measurements on the grounding testbed. The incorporation of measured S-parameters into a complete power systems simulation should also be envisaged. Furthermore, presently the ship hull is considered to be a perfect electric conductor. This means that each subsystem is ideally grounded. This does not correspond to reality. A single ground potential for all components of the power system does not take into account wave propagation along the ship hull structure. In future the presence of the metallic ship hull needs to be appropriately taken into consideration. It is believed that the ship hull structure has substantial impact to grounding characteristics such as voltage transients in the presence of a system fault. Additional voltage drops can occur due to large hull currents, which would further affect the local ground potential. Based on the S-parameter approach the ship hull needs to be considered as a multiport network as well (Figure 4.1).

Finally it is planned for 2013 to publish a paper on this topic in the IEEE Transactions on Power Delivery.



(a) Simplified grounding model: Each block is connected to an ideal ground that is on the same potential for all blocks



(b) Complete grounding model: Each block is grounded by a local connection to the ship hull. The ship hull assumes ground potential at a single location only (“super ground”). The ship hull itself is considered to be a multi-port network.

Figure 4.1: Characterization of common DC shipboard power distribution systems components based on S-parameters. Presently ship hull is considered to be a perfect electric conductor (above). Considering the presence of the metallic ship hull results in an additional multi-port network and regarding the system components in an additional port (below). Each block represents a linear time-invariant (LTI) network defined by S-parameters.

# List of Figures

1.1	Simplified shipboard power system comparing a conventional design with a design based on IPS . . . . .	5
1.2	Next Generation Integrated Power System (NGIPS) Technology Development Roadmap . . . . .	6
2.1	Simplified DC distribution system showing four different locations for potential faults . . . . .	10
2.2	Transient phenomena and system offset for a high grounding impedance	11
2.3	Common components of a simplified DC distribution system considered as multiport (N-port) networks . . . . .	13
3.1	Arbitrary N-port network . . . . .	17
3.2	Signal flow graph representation of a 2-port network . . . . .	20
3.3	2-port vector network analyzer (VNA) Agilent 8753ES . . . . .	23
3.4	Measurement system for $s_{11}$ and $s_{21}$ S-parameters using a 2-port vector network analyzer (VNA) [24, p. 189] . . . . .	24
3.5	Submatrices of a 4-port network obtained by 2-port measurements . .	25
3.6	Different measurement combinations of a 4-port network using a 2-port vector network analyzer (VNA) . . . . .	26
3.7	Power electronics of the experimental small-scale testbed used for grounding studies at Purdue University . . . . .	28
3.8	Measurements of the reflection coefficient $s_{33}$ of the DC/DC converter	29
3.9	Measured transmission coefficient $s_{34}$ of the DC/DC converter . . . .	30
3.10	Comparison between the frequency response of the rational function object and that of the original data . . . . .	33

3.11 Simulink model of a rational function object representing a single S-parameter . . . . .	34
3.12 S-parameters model block built in Simulink/SimPowerSystems . . . . .	36
3.13 Internals of the 2-port S-parameters model block . . . . .	36
3.14 Validation circuit designed in Agilent Design Software (ADS) . . . . .	38
3.15 Step response of the 4-port network used for the validation process . . . . .	39
3.16 Transmission line model of a monopolar DC distribution bus using lumped elements . . . . .	41
3.17 Simulation model of a capacitively grounded bipolar DC distribution bus with integrated S-parameter blocks . . . . .	41
3.18 Simulation result of the transmission line model implemented in Simulink/SimPowerSystems . . . . .	42
3.19 Simplified capacitively grounded bipolar DC distribution bus including the DC/DC converter S-parameters model . . . . .	43
3.20 Simulation result of the DC/DC converter model implemented in Simulink/SimPowerSystems . . . . .	44
4.1 Characterization of common DC shipboard power distribution systems components based on S-parameters . . . . .	49
A.1 Screenshot of the \\plasma\STUDENT\kofler directory at the PLASMA Server at CAPS . . . . .	62
B.1 Screenshot of the main GUI recommended to execute the tools built . . . . .	63
B.2 GUI of rational fitting tool used to build the S-parameter rational function models . . . . .	65
B.3 GUI of the plot tool developed to read Touchstone files and plot S-parameter data . . . . .	67
B.4 GUI of the tool designed to generate the Touchstone files of the measurements obtained with the 2-port VNA Agilent 8753ES . . . . .	69
B.5 GUI of the tool developed to assemble the partial 2-port measurements to a Touchstone file . . . . .	71
C.1 Screenshot of the mask of the S-parameter block . . . . .	73

C.2	Screenshot of the mask of the S-parameter transfer function blocks . . . . .	73
C.3	Screenshot of the „Parameter“ tab in the mask editor of the S-parameters block . . . . .	74
C.4	Screenshot of the „Initialization“ tab in the mask editor of the S-parameter transfer function blocks . . . . .	74
C.5	Screenshot of the model properties defined in Simulink . . . . .	75

# List of Tables

3.1	Required measurements of a N-port network using a 2-port VNA . . .	26
3.2	Number of rational transfer function blocks needed to implement a N-port network into a time domain circuit simulation . . . . .	36
3.3	Simulation parameters used for validation . . . . .	38
3.4	Simulation parameters used for the transmission line model simulation	40
3.5	Simulation parameters used for the DC/DC converter model simulation	43
3.6	Solver settings used for the simulations performed in Simulink/SimPowerSystems . . . . .	46
B.1	Number of CSV text files obtained measuring a N-port network by means of the 2-port VNA Agilent 8753ES . . . . .	68
D.1	Measurement combinations of a 3-port network using a 2-port VNA .	76
D.2	Measurement combinations of a 4-port network using a 2-port VNA .	77
D.3	Measurement combinations of a 5-port network using a 2-port VNA .	78
D.4	Measurement combinations of a 6-port network using a 2-port VNA .	79

# List of Abbreviations

AC	Alternating Current
AES	All Electric Ship
DC	Direct Current
DUT	Device Under Test
EMC	Electromagnetic Compatibility
EMI	Electromagnetic Interference
ESRDC	Electric Ship Research and Development Consortium
FEM	Finite Element Model
FSU	Florida State University
HFAC	High Frequency Alternating Current
IFFT	Inverse Fast Fourier Transform
IPS	Integrated Power System
LTI	Linear Time Invariant
MVAC	Medium Voltage Alternating Current
MVDC	Medium Voltage Direct Current
NGIPS	Next Generation Integrated Power System
ONR	Office of Naval Research
PCM	Power Converter Modules
PED	Power Electronic Device

RF	Radio Frequency
SL	Service Loads
U.S.	United States
VNA	Vector Network Analyzer
ZED	Zonal Electrical Distribution

# Bibliography

- [1] B. Wagner. (Nov. 2007) All-Electric Ship Could Begin to Take Shape By 2012. National Defense Magazine Archive. [Online]. Available: <http://www.nationaldefensemagazine.org/archive/2007/November/Pages/All-Electric2453.aspx> [Accessed: November 2, 2012]
- [2] P. B. Backlund, C. C. Seepersad, and T. M. Kiehne. A System-Level Design Framework for All-Electric Ship Thermal Systems. [Online]. Available: [https://www.navalengineers.org/ProceedingsDocs/EMTS2012/Papers/49\\_Backlund\\_EMMS2012Paper.pdf](https://www.navalengineers.org/ProceedingsDocs/EMTS2012/Papers/49_Backlund_EMMS2012Paper.pdf) [Accessed: December 10, 2012]
- [3] S. Littlefield and A. Nickens. (Feb. 15, 2005) Roadmap for the all-electric warship. Power Business and Technology for the Global Generation Industry. [Online]. Available: [http://www.powermag.com/renewables/wind/Roadmap-for-the-all-electric-warship\\_1044.html](http://www.powermag.com/renewables/wind/Roadmap-for-the-all-electric-warship_1044.html) [Accessed: December 10, 2012]
- [4] N. H. Doerry and J.C. Davis. (May 1994) Integrated Power System for Marine Applications. Naval Engineers Journal. [Online]. Available: <http://www.doerry.org/norbert/papers/ASNE1994DoerryAndDavis.pdf> [Accessed: December 2, 2012]
- [5] N. Doerry. (2009) Next Generation Integrated Power Systems for the Future Fleet. [Online]. Available: <http://www.doerry.org/norbert/papers/090106usna-ngips-final.pdf> [Accessed: December 2, 2012]
- [6] T. J. McCoy, "Trends in Ship Electric Propulsion," *IEEE Power Engineering Society Summer Meeting*, vol. 1, pp. 343–346, 25 Jul. 2002.
- [7] G. Buja, A. da Rin, R. Menis, and G. Sulligoi, "Dependable Design Assessment of Integrated Power Systems for All Electric Ships," *Electrical Systems for Aircraft, Railway and Ship Propulsion (ESARS)*, no. 1-8, 19-21 Oct. 2010.
- [8] V. R. Basam and A. Das. (2010) All Electric Ship-The Super Platform for Tomorrow's Naval Warfare. Second International

- Seminar and Exhibition on Naval Armaments. [Online]. Available: [http://www.researchgate.net/publication/209434238\\_All\\_Electric\\_Ship\\_-\\_The\\_Super\\_Platform\\_for\\_Tomorrow's\\_Naval\\_Warfare](http://www.researchgate.net/publication/209434238_All_Electric_Ship_-_The_Super_Platform_for_Tomorrow's_Naval_Warfare) [Accessed: December 2, 2012]
- [9] Capt. N. Doerry. Open Architecture Approach for the Next Generation Integrated Power System. [Online]. Available: <https://www.navalengineers.org/SiteCollectionDocuments/2007%20Proceedings%20Documents/Automation%20and%20Controls%202007/1-2-9%20Paper.pdf> [Accessed: December 2, 2012]
- [10] L. HanYu and M. LongHua, "Integrated Protection on Shipboard Integrated Power System," *International Conference on Advanced Power System Automation and Protection (APAP)*, vol. 1, pp. 252–255, 16-20 Oct. 2011.
- [11] K. P. Logan, "Intelligent Diagnostic Requirements of Future All-Electric Ship Integrated Power System," *Industry Applications Society 52nd Annual Petroleum and Chemical Industry Conference*, pp. 151–163, 12-14 Sep. 2005.
- [12] L. Petersen (POI). (Aug. 2008) Next Generation Integrated Power Systems. ONR Program Code 33. [Online]. Available: <http://www.onr.navy.mil/~media/Files/Fact%20Sheets/Next%20Generation%20Integrated%20Power%20Supply.ashx> [Accessed: December 10, 2012]
- [13] B. Jacobson and J. Walker, "Grounding Considerations for DC and Mixed DC and AC Power Systems," *Society of Naval Engineers Journal*, vol. 119, no. 2, pp. 49–62, Oct. 2007.
- [14] Y. Pen, P. M. Silveira, M. Steurer, T.L Baldwin, and P. F. Ribeiro, "A Fault Location Approach for High-Impedance Grounded DC Shipboard Power Distribution Systems," *IEEE Power and Energy Society General Meeting - Conversion and Delivery of Electrical Energy in the 21st Century*, no. 1-6, 20-24 Jul. 2008.
- [15] IEEE Std. 45, "IEEE Recommended Practice for Electrical Installations on Shipboard," *IEEE Industry Applications Society*, pp. 1–258, 2002.
- [16] IEEE Std. 142 (Green Book), "IEEE Recommended Practice for Grounding of Industrial and Commercial Power Systems," pp. 1–135, 17 Sep. 1982.
- [17] Y. Nyanteh, L. Graber, C. Edrington, S. Srivastava, and D. Cartes, "Overview of Simulation Models for Partial Discharge and Electrical Treeing to Determine

- Feasibility for Estimation of Remaining Life of Machine Insulation Systems,” *Electrical Insulation Conference (EIC)*, pp. 327–332, 5-8 Jun. 2011.
- [18] D. Infante, J. Langston, L. Graber, and M. Steurer, “Guiding the Selection of Physical Experiments Supporting Validation of Electric Power System Models,” *Conference on Grand Challenges in Modeling & Simulation*, pp. 173–180, 2011.
- [19] D. Lee, D. Infante, J. Langston, S. V. Poroseva, M. Steurer, and T. Baldwin, “Grounding Studies in a Medium Voltage DC Shipboard Power System with Uncertain Parameters,” *Conference on Grand Challenges in Modeling & Simulation*, pp. 113–120, 2010.
- [20] L. Graber, D. Infante, M. Steurer, and W.W. Brey, “Model Validation for Shipboard Power Cables Using Scattering Parameters,” *High Voltage Engineering*, vol. 37, no. 11, pp. 2836–2842, 2011.
- [21] V. Cecchi, A. Leger, and K. Miu, “Modeling Approach for Transmission Lines in the Presence of Non-Fundamental Frequencies,” *IEEE Transactions on Power Delivery*, vol. 24, no. 4, pp. 2328–2335, Oct. 2009.
- [22] H. W. Dommel, “Digital Computer Solution of Electromagnetic Transients in Single-and Multiphase Networks,” *IEEE Transactions on Power Apparatus and Systems*, vol. PAS-88, no. 4, pp. 388–399, Apr. 1969.
- [23] D. M. Pozar, *Microwave and RF Design of Wireless Systems*. New York and Chichester: Wiley, 2000.
- [24] R. Ludwig and P. Bretchko, *RF Circuit Design: Theory and Applications*. Upper Saddle River: Prentice Hall, 2000.
- [25] J. A. Dobrowolski, *Microwave Network Design Using the Scattering Matrix*. Boston: Artech House, 2010.
- [26] K. Kurokawa, “Power Waves and the Scattering Matrix,” *IEEE Transactions on Microwave Theory and Techniques*, vol. 13, no. 2, pp. 194–202, Mar. 1965.
- [27] E.W. Matthews, “The Use of Scattering Matrices in Microwave Circuits,” *IRE Transactions on Microwave Theory and Techniques*, vol. 3, no. 3, pp. 21–26, Apr. 1955.
- [28] L. G. Maloratsky, *Passive RF & Microwave Integrated Circuits*. Amsterdam and Bosto: Elsevier/Newnes, 2004.
- [29] S. Ramo, J. R. Whinnery, and T. van Duzer, *Fields and Waves in Communication Electronics*, 3rd ed. New York: John Wiley & Sons, 1994.

- [30] D. A. Frickey, "Conversions Between S, Z, Y, h, ABCD, and T Parameters which are Valid for Complex Source and Load Impedances," *IEEE Transactions on Microwave Theory and Techniques*, vol. 42, no. 2, pp. 205–211, Feb. 1994.
- [31] W. Rivas-Torres. (March 2006) Using S-parameter data effectively. EE Times-India. [Online]. Available: <http://www.eetimes.com/design/microwave-rf-design/4009625/Using-S-parameter-data-effectively> [Accessed: January 14, 2013]
- [32] B. Brunn. (Feb. 2005) Proposal for S-parameter Extrapolation to DC. [Online]. Available: [http://www.ieee802.org/3/ap/public/channel\\_adhoc/brunn\\_c1\\_0305.pdf](http://www.ieee802.org/3/ap/public/channel_adhoc/brunn_c1_0305.pdf) [Accessed: January 14, 2013]
- [33] W. T. Beyene and J. E. Schutt-Aine, "Efficient Transient Simulation of High-Speed Interconnects Characterized by Sampled Data," *IEEE 5th Topical Meeting, Electrical Performance of Electronic Packaging*, pp. 162–165, 28-30 Oct 1996.
- [34] H. Shi, "A Refinement Procedure for S-Parameter DC Extrapolation based on Sampling Theorem and Causality," *IEEE Electrical Performance of Electronic Packaging*, pp. 43–46, 29-31 Oct. 2007.
- [35] J. Schutt-Anie, J. Tan, C. Kumar, and F. Al-Hawari, "Blackbox Macromodel with S-Parameters and Fast Convolution," *12th IEEE Workshop on Signal Propagation on Interconnects*, pp. 1–4, 12-15 May 2008.
- [36] R. X. Zeng, "Modified Rational Function Modeling for Multi-Port High-Speed Differential Circuits," *International Conference on Microwave and Millimeter Wave Technology (ICMMT)*, vol. 2, pp. 459–462, 21-24 Apr. 2008.
- [37] D. Benson. The MathWorks, Inc.. Email Correspondence between May and September 2012.
- [38] EIA/IBIS Open Forum. Touchstone File Format Specification: Rev. 1.1, 2002. [Online]. Available: ([http://www.vhdl.org/pub/ibis/connector/touchstone\\_spec11.pdf](http://www.vhdl.org/pub/ibis/connector/touchstone_spec11.pdf)) [Accessed: November 10, 2012]
- [39] VNA Agilent 8753ES. [Online]. Available: [http://www.testunlimited.com/images/products/agilent\\_8753es.jpg](http://www.testunlimited.com/images/products/agilent_8753es.jpg) [Accessed: December 5, 2012]
- [40] J.C. Tippet and R.A. Speciale, "A Rigorous Technique for Measuring the Scattering Matrix of a Multiport Device with a 2-Port Network Analyzer," *IEEE Transactions on Microwave Theory and Techniques*, vol. 30, no. 5, pp. 661–666, May 1982.

- [41] The MathWorks Inc. Matlab 7.9.1 Service Pack 1 (R2009b SP1). (2012). [Online]. Available: <http://www.mathworks.com> [Accessed: November 11, 2012]
- [42] R. X. Zeng and J. H. Sinsky, "Modified Rational Function Modeling Technique for High Speed Circuits," *IEEE MTT-S Int. Microwave Microwave Symposium Digest*, pp. 1951–1954, 11-16 Jun. 2006.
- [43] B. Gustavsen and A. Semlyen, "Rational Approximation of Frequency Domain Responses by Vector Fitting," *IEEE Transactions Power Delivery*, vol. 14, no. 3, pp. 1051–1061, Jul 1999.
- [44] C. Warwick. (August 2007) Using model-based design in signal integrity engineering. EE Times-India. [Online]. Available: [http://www.eetindia.co.in/STATIC/PDF/200708/EEIOL\\_2007AUG01\\_RFD\\_EDA\\_EMS\\_NETD\\_SIG\\_TA\\_01.pdf?SOURCES=DOWNLOAD](http://www.eetindia.co.in/STATIC/PDF/200708/EEIOL_2007AUG01_RFD_EDA_EMS_NETD_SIG_TA_01.pdf?SOURCES=DOWNLOAD) [Accessed: January 14, 2013]
- [45] L. W. Nagel and D.O. Pederson. (April 1973) SPICE (Simulation Program with Integrated Circuit Emphasis). [Online]. Available: <http://www.eecs.berkeley.edu/Pubs/TechRpts/1973/22871.html> [Accessed: December 27, 2012]
- [46] Agilent Design Software ADS 2011.10. (2012). [Online]. Available: <http://www.home.agilent.com/agilent/software.jsp?ckey=2212036&lc=eng&cc=US&nid=-34335.0&id=2212036&pageMode=PV> [Accessed: November 11, 2012]
- [47] W. Rivas-Torres. Agilent Technologies, Inc.. Email Correspondence 19 September 2012 (CaseID 1049432).
- [48] The MathWorks. (2012) Documentation Center. [Online]. Available: <http://www.mathworks.com/help> [Accessed: December 15, 2012]
- [49] K. Schoder. Center for Advanced Power Systems (CAPS). Private Communication.

# A Archiving

The research presented in this thesis has been performed at the Center for Advanced Power Systems (CAPS) in 2012. As a result of the research, a range of documents, scripts and simulation files have been created. This appendix gives an overview what is available, so other students and ESRDC members can use the result for further investigations. All the files which have been created while working on this project are stored in the student directory on the PLASMA-Server at CAPS. The full path to access the files is `\\plasma\STUDENT\kofler`.

**1\_ Work:** Scripts and simulations files made in MATLAB/Simulink and Agilent Design Software (ADS). Also includes the Comsol models and Touchstone files as well as MATLAB tools.

**2\_ Presentations:** Presentation for the National High Magnetic Field Laboratory (NHMFL) Seminar 2012, the ESRDC Meeting presentation, a range of presentations for bi-weekly teleconferences with Purdue University and the final presentation presented at the power system group meeting.

**3\_ Other:** All third party files which were necessary and helpful to obtain this project such as literature, datasheets, specifications, drawings, orders, etc.

**4\_ Support:** Important email conversation (as PDF) and the files interchanged

Figure A.1 shows a screenshot of the tree structure of the directory.

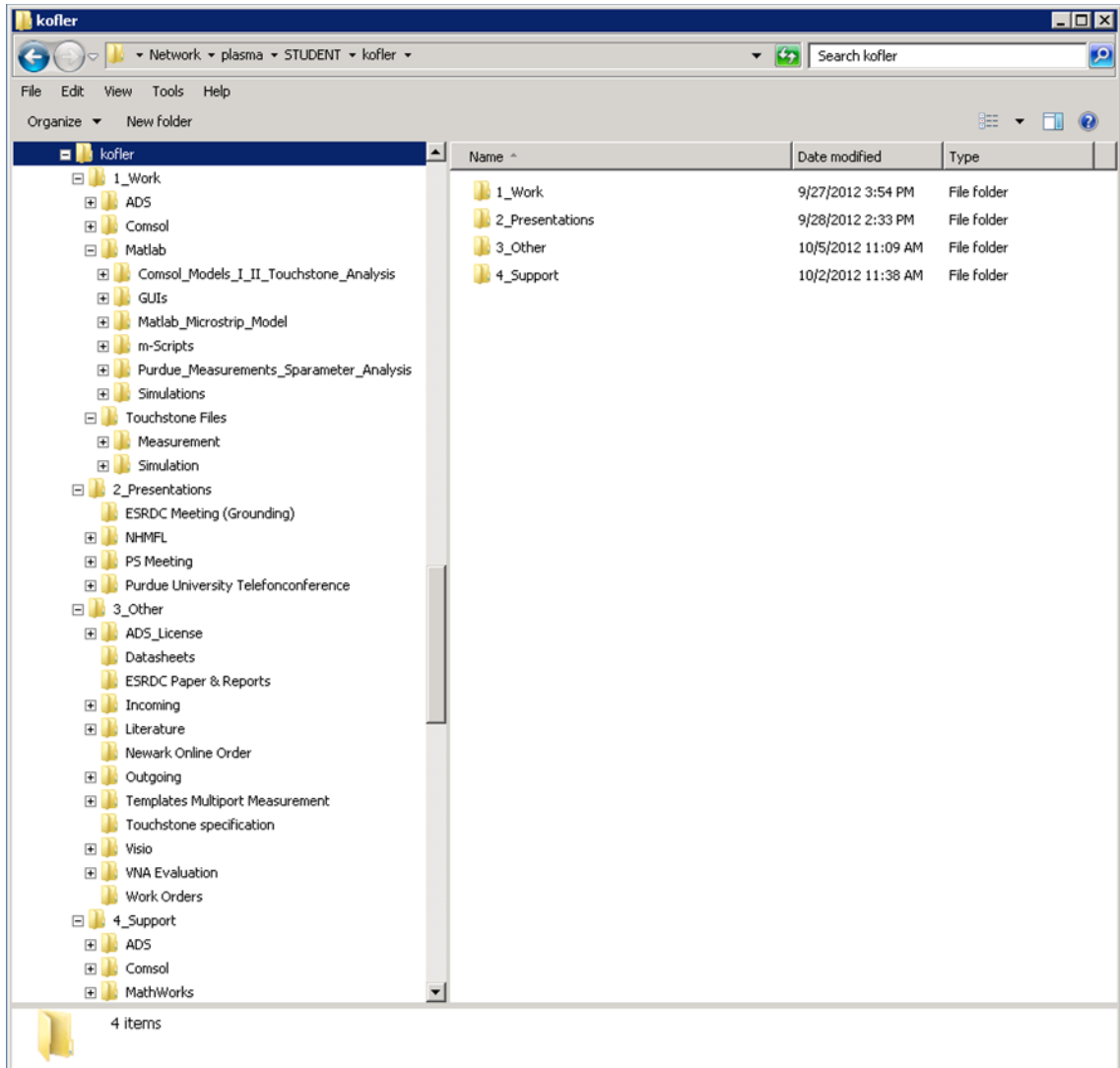


Figure A.1: Screenshot of the \\plasma\STUDENT\kofler directory at the PLASMA Server at CAPS

# B MATLAB Tools

This appendix is a comprehensive summary of the implemented tools which support the overall S-parameters approach. Four Graphical User Interfaces (GUIs) have been built. Their particular purpose will be described in the following. The tools can be found in the directory \\plasma\1\_Work\Matlab\GUIs.

## B.1 Main GUI

It is recommended to execute the individual tools by the main GUI shown in Figure B.1. This GUI can be executed either by the `OpenGUI.m` or the stand-alone application `GUIs_CAPS.exe` located in the EXE folder. Note that the latter requires the Matlab Compiler Runtime (MCR) installed (version 7.15 or higher).

**Remark:** In case of not using the stand-alone application, the tools created require an installed version of the RF Toolbox (Version 2.6 (MATLAB 2009) or higher).

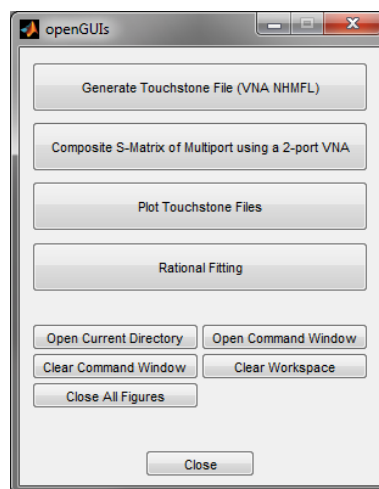


Figure B.1: Screenshot of the main GUI recommended to execute the tools built

## B.2 Rational Fitting for S-parameter Transfer Functions

### Description

Figure B.2 shows the Matlab GUI for the rational fitting process needed to build the S-parameters rational function models. The fitting algorithm used fits a rational function model (Eq. 3.11) to the complex input data in the specified frequency range. The input data is stored in a Touchstone file that contains N-port S-parameters. The important input parameters which need to be specified are the fitting error tolerance `tol` in [dB], the asymptotic behavior of the fit `tendstozero`, the delay factor `delayfactor` and the number of poles `npoles`. The result of the approximation is a `<NxN rfmodel.rational>` object with the properties A (poles), C (residues), D (direct feed) and Delay. It also determines the number and order of transfer function blocks for each S-parameter needed. Finally the fit can be stored in a MAT-file (\*.mat).

### How To Use

1. Add the Touchstone file that contains N-port S-parameters (\*.sNp).
2. Press the button „Get Data“ to load the complex data.
3. Specify the rational fitting parameters values. The default values do the job very well in many cases but may need to be adjusted on a case by case basis. To set the tolerance and poles manually may result in that the number of poles does not gain the desired tolerance. Manually setting these input parameters is (only) recommended if the order of the system is known (e.g. lumped element models) [37]. To obtain an accurate fit, the rule of thumb is to choose the number of poles greater than or at least equal to twice the number of observable peaks on a plot of the data in the frequency domain [48, "rationalfit"]. Providing a tolerance value and set the number of poles to [] (bracket) and let the fitting algorithm determine the required order of the system is typically recommended for measurement data on distributed systems where determining the order of the system is non-trivial [37]. It may results in a higher number of transfer function blocks (stages) used to implement the rational function object for a single S-parameter.
4. Apply curve fitting function to the input data. The fit can be applied to all N-port S-parameters automatically using the same input parameter values

by checking the checkbox „Fit all“. Otherwise the S-parameters can be fitted manually using different input parameter values for each S-parameter.

5. Save the rational function object to a MAT-file (\*.mat). The rational function object can only be saved if the fit is applied to all  $N^2$  S-parameters.

### Remarks

The tool is built using MATLAB 2009b but the fitting function of MATLAB 2011a implemented. It turned out that the fitting algorithm of the 2009b version does not achieve the same accuracy as versions 2009b SP1 and higher in some cases using the same input parameters. The time needed to fit the complex frequency domain data depends on the computer hardware, the fitting tolerance, the number of poles, the number of data points etc.

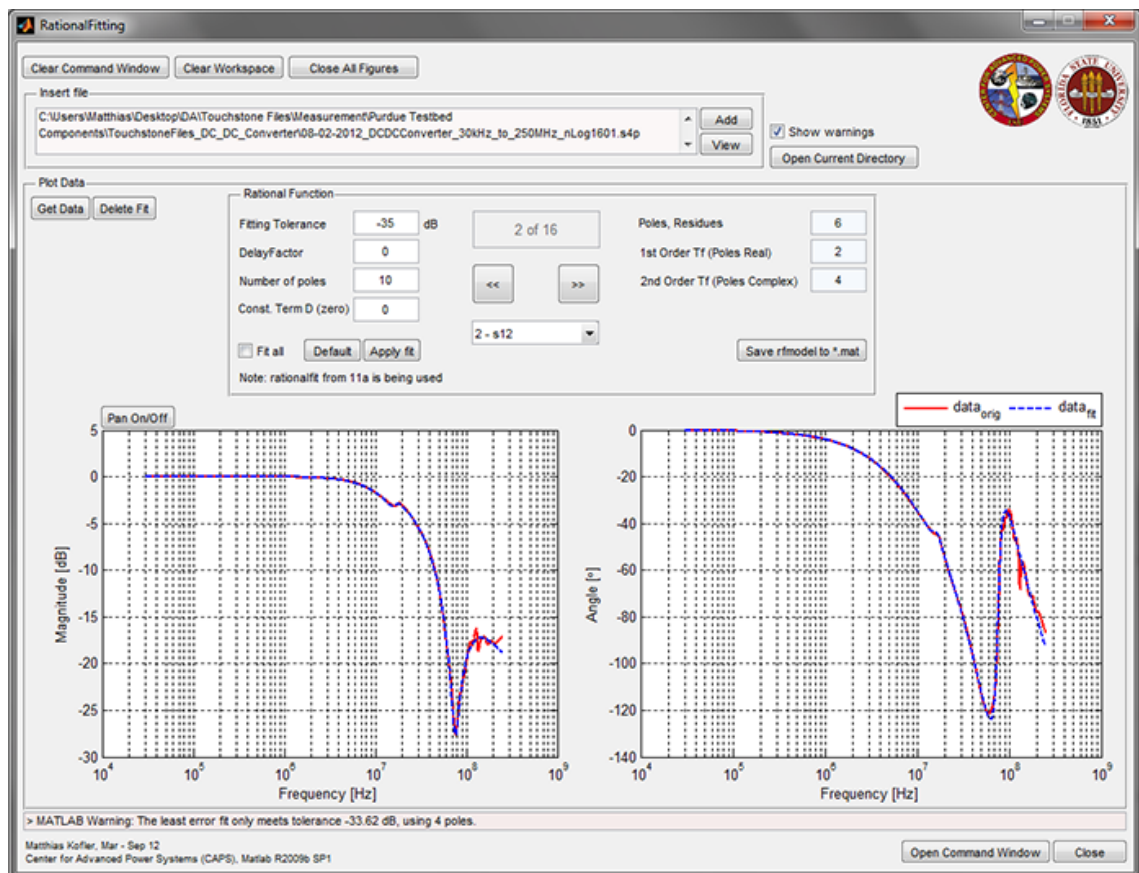


Figure B.2: GUI of rational fitting tool used to build the S-parameter rational function models

## B.3 Visualization of S-parameter data

### Description

The interpretation of S-parameters might be needed case-by-case. To achieve this in a simple and less time-consuming manner, a tool has been built which allows to efficiently plot S-parameter data. The tool not only allows to plot S-parameter data but also alternative network parameters such as Z- or Y-parameters. It provides the capability to display the input data in linear and logarithmic form as well as in polar coordinates (S-parameters only). In certain cases it may be sufficient to plot just a few of the network parameters. This can be done by checking the checkbox of the corresponding network parameter. The number of added files is equal to the number of line objects in one figure present. The total number of figures created depends on the network parameters chosen. In addition to this, the tool offers a couple of settings to specify the most important plot properties. The properties are applied to a selected line object in all figures present. In order to prevent the addition of Touchstone files with distinct extension and hence a possible mismatch due to a different number of N-port S-parameters, a filter has been implemented. The filter is set once the selection in the panel „Select Network“ is made. Open figures can be saved.

### How To Use

1. Select a network in the panel „Select Network“.
2. Add the files to be plotted.
3. Choose the display form desired, the parameters as well as the format. Select the network parameter of interest (Checkboxes).
4. To display the input data press „Plot“.
5. Optional: Define the plot properties.
6. Optional: Press the „Save Figures“ button to save the figures opened.

### Remarks

Some of the plot properties are applied on-the-fly to the figures and line objects present. The figures created are provided with a tag. In the event of saving the figures present, figures of other MATLAB entities will be excluded.

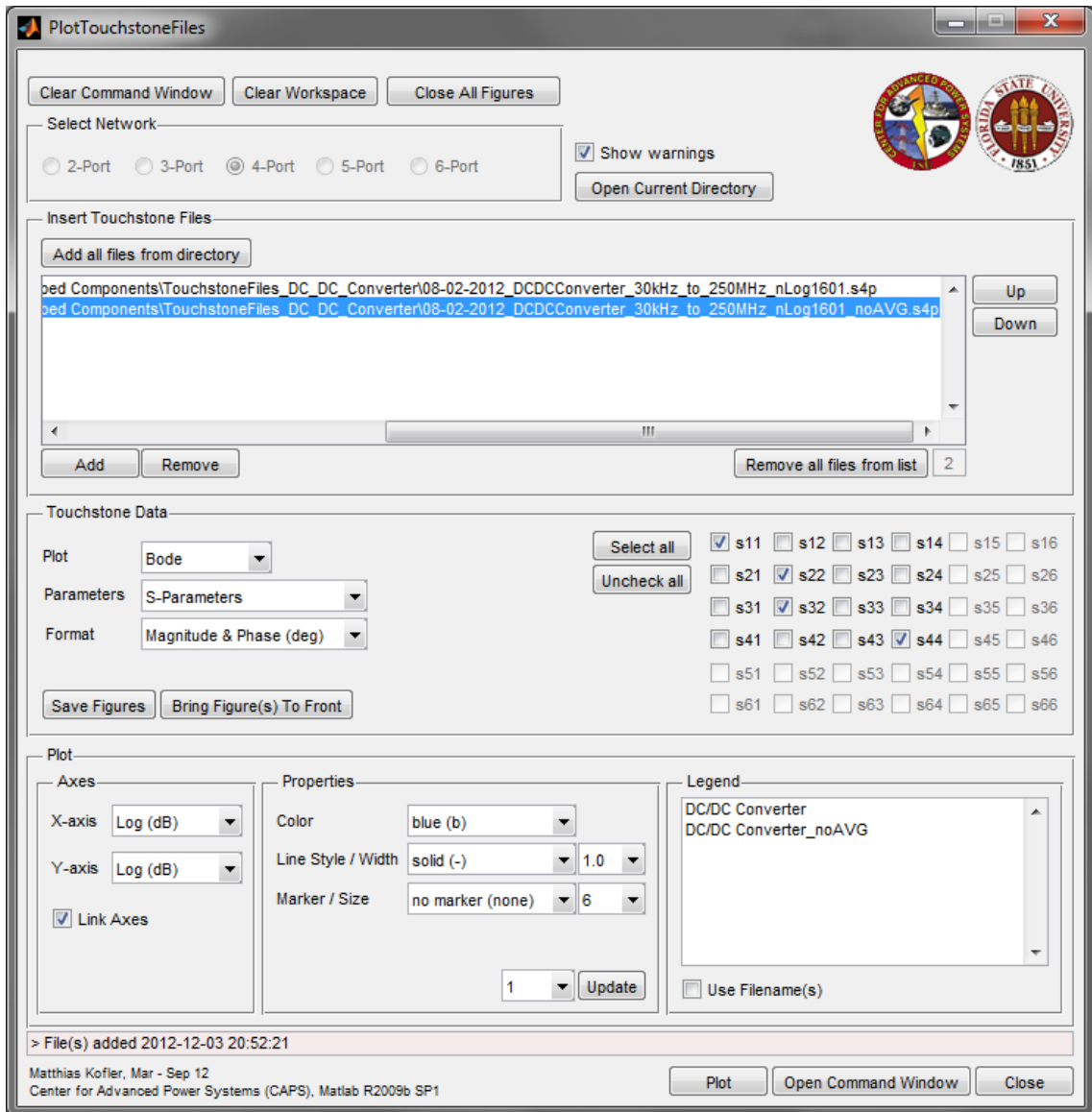


Figure B.3: GUI of the plot tool developed to read Touchstone files and plot S-parameter data

## B.4 Generation of Touchstone<sup>®</sup>-File

### Description

The 2-port vector network analyzer (VNA) Agilent 8753ES available at the National High Magnetic Field Laboratory (NHMFL) that was used in this work does not support to output Touchstone files. Instead the VNA exports each of the four S-parameters in a CSV text file format respectively. A single measurement results in eight \*.csv text files in total, since the magnitude and phase data is stored in separate files respectively. Following the approach to characterize a multiport network by means of a 2-port VNA this results in a large number of CSV files as can be seen in table B.1.

N-port	2-port	3-port	4-port	5-port	6-port
Number of CSV files	8	24	48	80	120

Table B.1: Number of CSV text files obtained measuring a N-port network by means of the 2-port VNA Agilent 8753ES

To obtain the Touchstone file(s) desired it would be very tedious and time-consuming to merge all the single files manually. To complete this task as effortless and fast as possible, a tool has been established which makes the compilation automatically. The only part which needs to be done manually is to insert the necessary files in the correct order. The result is a Touchstone file which meets the requirements defined in the specification [38].

### How To Use

1. Choose the File Format (\*.csv default)
2. Add the text files that contain the magnitude and phase data of the measured S-parameters. It is important to insert the files in the right order (the default order is displayed below the listbox).
3. In the panel „Touchstone Files“ a couple of settings can be made such as the Option Line desired. The Option Line defines the format of the S-parameters finally stored in the Touchstone file. If everything is set as requested, push the button „Write Touchstone File“ to generate the Touchstone file. Additionally, a saving dialog appears which allows to save the generated Touchstone file (\*.s2p) in the chosen directory.

### Remarks

Depending on the computer performance the merging procedure may takes a few seconds. Furthermore, the S-parameters donation in the CSV text files is independent of the corresponding measurement and always equal. The same applies to the generated Touchstone file for technical reasons. Hence it is recommended to add a comment to the Touchstone file and note the actual S-parameters to which the given ones are equivalent to.

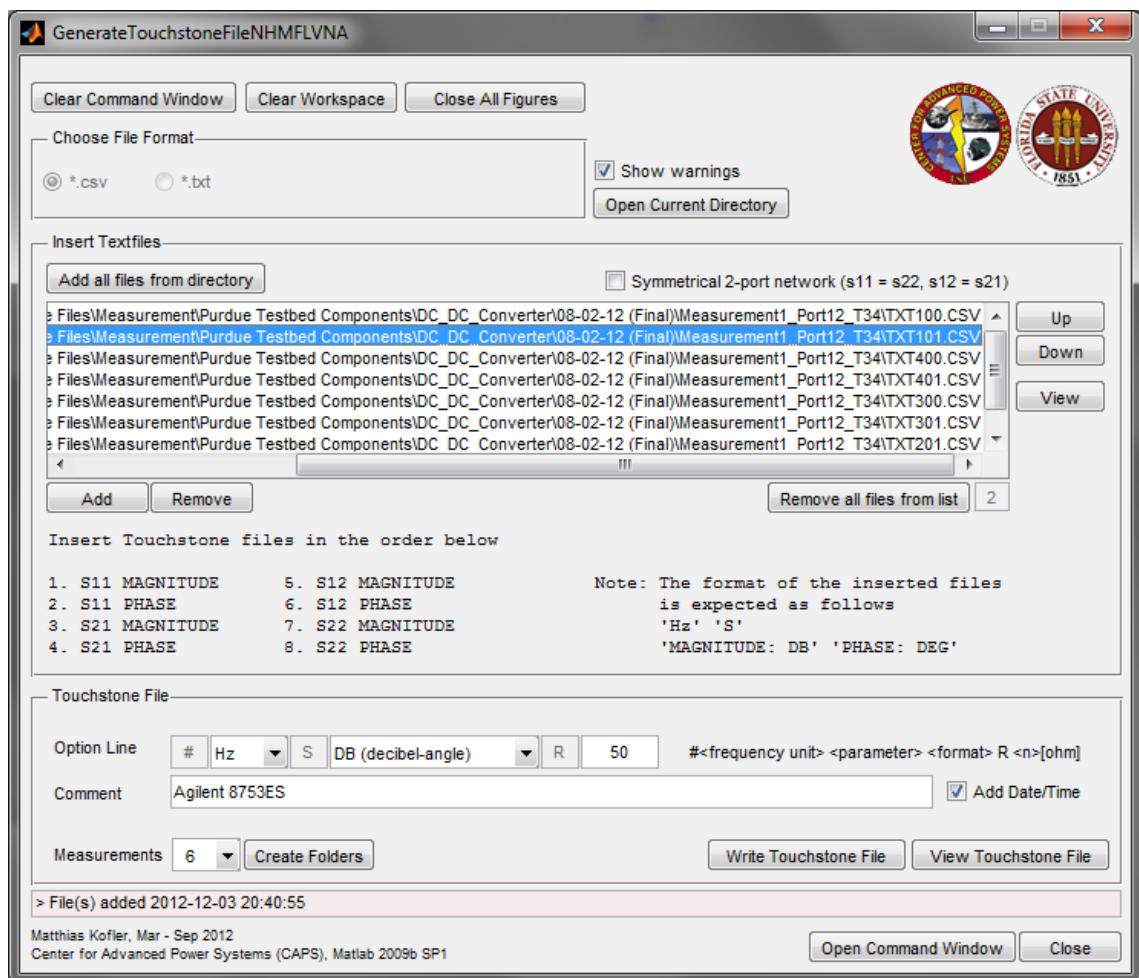


Figure B.4: GUI of the tool designed to generate the Touchstone file(s) of the measurements obtained with the 2-port VNA Agilent 8753ES at the National High Magnetic Field Laboratory (NHMFL)

## B.5 Assembling of the N-Port S-Matrix

### Description

In section 3.3 it has been described how to obtain S-parameters of an N-port network by means of a 2-port VNA. The result is a number of Touchstone files (\*.s2p) which need to be assembled to a single Touchstone file (\*.sNp). To do this task manually can be very time-consuming and error-prone. Hence, a tool has been designed which makes this task as effortless as possible. The only part which needs to be done manually is to insert the necessary files in the correct order. The result is a Touchstone file which contains the entire S-parameter data needed to represent the N-port network measured.

### How To Use

1. Select the network in the panel „Select Network“.
2. Add all 2-port Touchstone files (\*.s2p) of the N-port network. It is vital to add the needed files in the correct order. To keep this task as manageable as possible, right below the listbox the adding steps are recorded. It can be seen which S-parameters are taken and needed to assemble the  $N \times N$  matrix. The expected order how to add the files is displayed below the listbox or can be found in Appendix D as well.
3. Define the Option Line desired. The Option Line defines how the S-parameters finally stored in the Touchstone file.
4. Select how duplicate elements (diagonal S-parameters) are handled: average or first available. Note that in literature there is no clear definition how to calculate the arithmetic mean of complex numbers. For this reason, the arithmetic mean of magnitude ( $r$ ) and phase ( $\theta$ ) of the complex frequency domain data ( $z$ ) of each of the diagonal S-parameters will be calculated respectively. They are converted to complex data using the statement  $z = re^{j\theta}$ . If unchecked, that diagonal S-parameter corresponding to the file inserted will be taken respectively.
5. Press „Write Touchstone File“ to generate the Touchstone file containing the N-port S-parameters.

### Remarks

Nothing to note

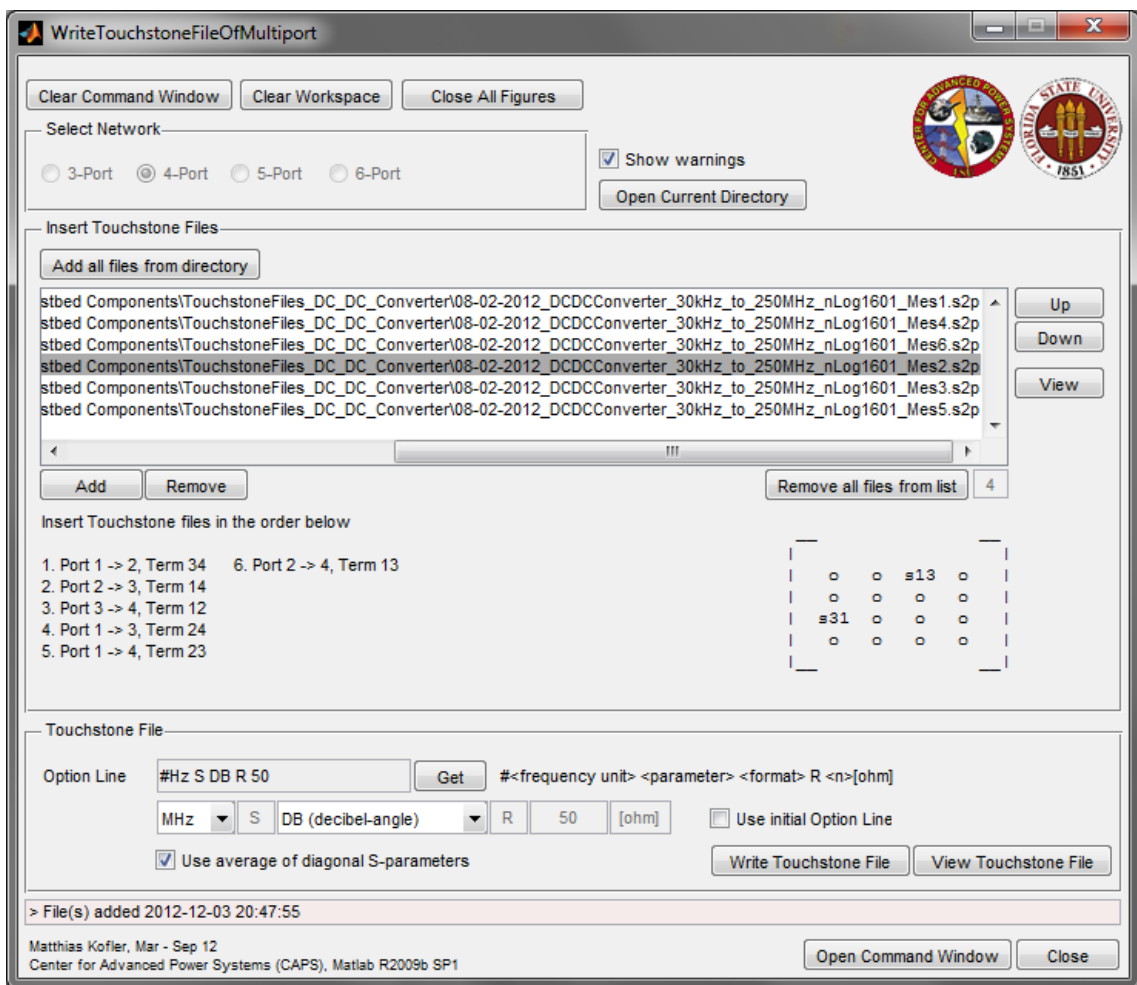


Figure B.5: GUI of the tool developed to assemble the partial 2-port measurements to a Touchstone file which containing the N-port S-parameters

# C S-parameters Model Description

This appendix gives an overview how the S-parameters block is implemented in Simulink/SimPowerSystems. The model implementation features two subsystems in total. One subsystem includes the transfer function blocks for each S-parameter needed and the necessary blocks to implement the equations that link the S-parameters to the input and output port voltage(s) and current(s). This subsystem is represented by the S-parameter block on the top-level. The second subsystem represents the transfer function block for each S-parameter respectively. It contains the necessary blocks to implement the corresponding rational function model respectively. The latter will be automatically built and/or manipulated by the execution of m-code.

The use of subsystems is recommended since it helps to reduce the number of blocks displayed in the model built and allows to link functionally related blocks. Moreover it enables to establish a hierarchical block diagram, where a subsystem block is on one layer and the blocks that assemble the subsystem are on another layer. The model is built from the lowest layer to the top layer but for description purposes it will be described in inverse order.

The option of masking a block has been used to change the appearance of a subsystem. Masking a block allows to add a customized interface to the corresponding subsystem and allows to set and change parameters used by the system underneath. Furthermore, it provides restricted access to data. This means it enables to only change the specific parameters of the masked block but not its underlying characteristics.

Double clicking on the S-parameters block on the top-level opens the mask as shown in Figure C.1.

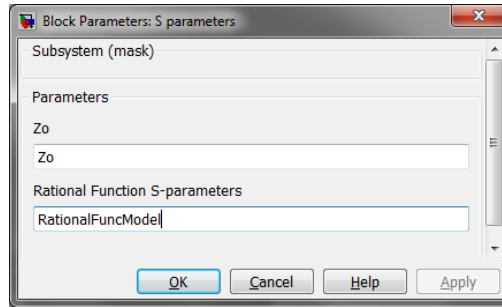


Figure C.1: Screenshot of the mask of the S-parameter block on the top-level

Two variables need to be defined and loaded into the workspace to use the S-parameters block in a circuit simulation. The reference impedance  $Z_0$  and the rational function model (rfmodel) of the DUT used for the simulation. The rf-model can be obtained by applying the rational fit algorithm to the original set of S-parameters of the DUT being considered. It is necessary to specify the variable names in the mask. Here, the rational function object is expected to be defined as `RationalFuncModel` in the workspace. The reference impedance is expected to be defined as `Zo`.

To view the internals of the S-parameter block the „Look under mask“ menu item needs to be used. This system uses the parameters specified in the mask. Each rational transfer function model block represents the S-parameters respectively. These provide a mask as well. To build the rational model the data of the variable `RationalFuncModel` is needed. In order to pick the data for each S-parameter individually the mask parameter is set to `RationalFunctionModel(i,j)` respectively. These masks also have an initialization callback (Figure C.4) that picks up this data and automatically builds the model using an external m-script called `build_simulink_model.m`. This script is called by each S-parameter transfer function block implemented in the subsystem.

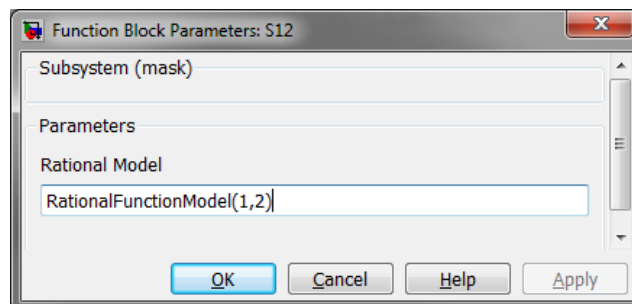


Figure C.2: Screenshot of the mask of the S-parameter transfer function blocks

Note: The variables being used are not equal. In the mask editor of the S-parameter block a new variable has been defined for the rational function object (Figure C.3).

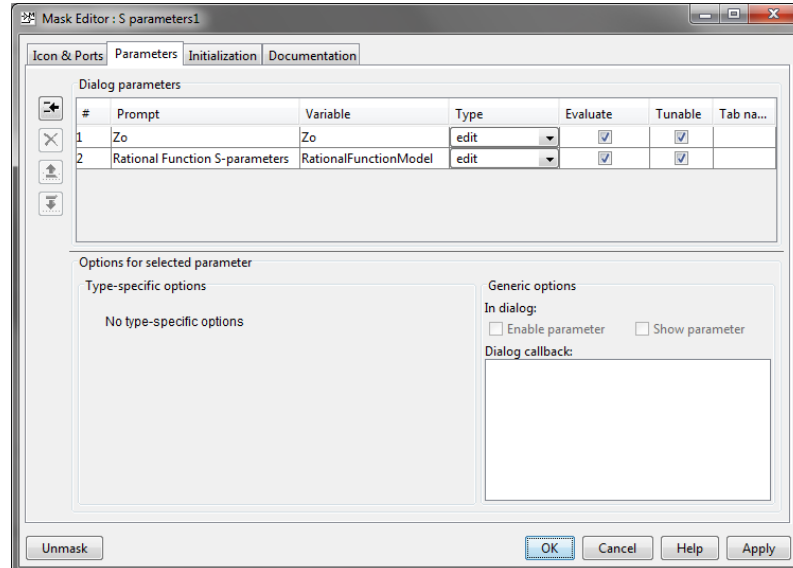


Figure C.3: Screenshot of the „Parameter“ tab in the mask editor of the S-parameters block

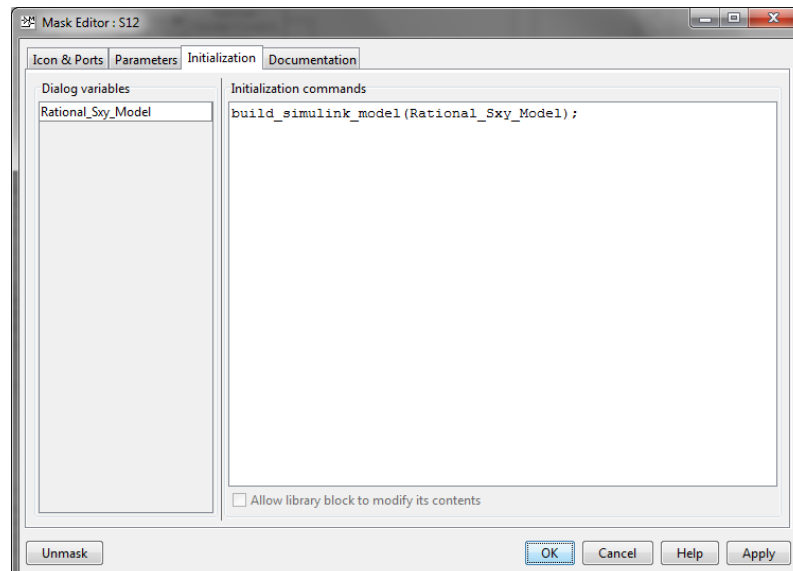


Figure C.4: Screenshot of the „Initialization“ tab in the mask editor of the S-parameter transfer function blocks

As a final note on the simulation topic. The usual way to parameterize a simulation model in Simulink is to define the necessary variables in a separate initialization script. This script is then executed line-by-line before starting the simulation. For

the simulations performed the initialization of the necessary variables is handled by opening a function callback (PreLoadFcn) in the model properties of the simulation model file (.mdl) as shown in Figure C.5. Then the defined variables will be automatically loaded into the workspace when the .mdl file is opened. In Simulink the function callback can be invoked at File → Model Properties → Callbacks → PreLoadFcn. In addition to this the simulation start and stop function is set by the stopwatch timer (tic, toc) to measure the actual simulation time.

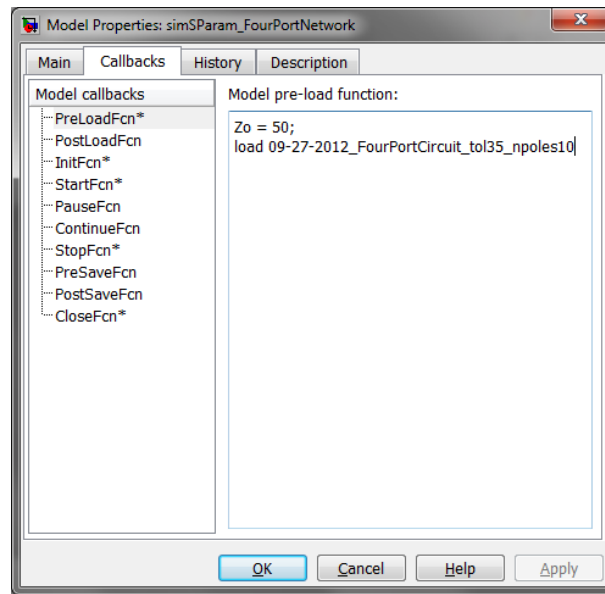


Figure C.5: Screenshot of the model properties defined in Simulink

The necessary files to run a simulation in Simulink including an S-parameter model are

1. simulation\_model\_file.mdl
2. build\_simulink\_model.m
3. NxN rfmodel.rational object containing the fitting data.

Note: For the simulations performed the data is stored in a \*.mat file (MM-DD-YY\_DUT\_tolX\_npolesX.mat) and attached to each simulation model respectively. The data appears in the workspace as a variable named „RationalFuncModel“ with the value <NxN rfmodel.rational>.

Then run the simulation. This approach is being used for all simulation models created.

# D Multiport Characterization using a 2-Port Network Analyzer

## D.1 3-Port Network Measurements

Number of measurements required: 3

#	Measurement	Partial S-Matrix	Insert Order into GUI (B.5)	Reconstructed S-Matrix
1	1 to 2 _ T3	$\begin{pmatrix} s_{11} & s_{12} \\ s_{21} & s_{22} \end{pmatrix}$	1	$\begin{pmatrix} s_{11} & s_{12} & s_{13} \\ s_{21} & s_{22} & s_{23} \\ s_{31} & s_{32} & s_{33} \end{pmatrix}$
2	1 to 3 _ T2	$\begin{pmatrix} s_{11} & s_{13} \\ s_{31} & s_{33} \end{pmatrix}$	3	
3	2 to 3 _ T1	$\begin{pmatrix} s_{22} & s_{23} \\ s_{32} & s_{33} \end{pmatrix}$	2	

Table D.1: Measurement combinations of a 3-port network using a 2-port VNA

## D.2 4-Port Network Measurements

Number of measurements required: 6

#	Measurement	Partial S-Matrix	Insert Order into GUI (B.5)	Reconstructed S-Matrix
1	1 to 2 _ T34	$\begin{pmatrix} s_{11} & s_{12} \\ s_{21} & s_{22} \end{pmatrix}$	1	$\begin{pmatrix} s_{11} & s_{12} & s_{13} & s_{14} \\ s_{21} & s_{22} & s_{23} & s_{24} \\ s_{31} & s_{32} & s_{33} & s_{34} \\ s_{41} & s_{42} & s_{43} & s_{44} \end{pmatrix}$
2	1 to 3 _ T24	$\begin{pmatrix} s_{11} & s_{13} \\ s_{31} & s_{33} \end{pmatrix}$	4	
3	1 to 4 _ T23	$\begin{pmatrix} s_{11} & s_{14} \\ s_{41} & s_{44} \end{pmatrix}$	5	
4	2 to 3 _ T14	$\begin{pmatrix} s_{22} & s_{23} \\ s_{32} & s_{33} \end{pmatrix}$	2	
5	2 to 4 _ T13	$\begin{pmatrix} s_{22} & s_{24} \\ s_{42} & s_{44} \end{pmatrix}$	6	
6	3 to 4 _ T12	$\begin{pmatrix} s_{33} & s_{34} \\ s_{43} & s_{44} \end{pmatrix}$	3	

Table D.2: Measurement combinations of a 4-port network using a 2-port VNA

### D.3 5-Port Network Measurements

Number of measurements required: 10

#	Measurement	Partial S-Matrix	Insert Order into GUI (B.5)	Reconstructed S-Matrix
1	1 to 2 _ T345	$\begin{pmatrix} s_{11} & s_{12} \\ s_{21} & s_{22} \end{pmatrix}$	1	$\begin{pmatrix} s_{11} & s_{12} & s_{13} & s_{14} & s_{15} \\ s_{21} & s_{22} & s_{23} & s_{24} & s_{25} \\ s_{31} & s_{32} & s_{33} & s_{34} & s_{35} \\ s_{41} & s_{42} & s_{43} & s_{44} & s_{45} \\ s_{51} & s_{52} & s_{53} & s_{54} & s_{55} \end{pmatrix}$
2	1 to 3 _ T245	$\begin{pmatrix} s_{11} & s_{13} \\ s_{31} & s_{33} \end{pmatrix}$	5	
3	1 to 4 _ T235	$\begin{pmatrix} s_{11} & s_{14} \\ s_{41} & s_{44} \end{pmatrix}$	6	
4	1 to 5 _ T234	$\begin{pmatrix} s_{11} & s_{15} \\ s_{51} & s_{55} \end{pmatrix}$	7	
5	2 to 3 _ T145	$\begin{pmatrix} s_{22} & s_{23} \\ s_{32} & s_{33} \end{pmatrix}$	2	
6	2 to 4 _ T135	$\begin{pmatrix} s_{22} & s_{24} \\ s_{42} & s_{44} \end{pmatrix}$	8	
7	2 to 5 _ T134	$\begin{pmatrix} s_{22} & s_{25} \\ s_{52} & s_{55} \end{pmatrix}$	9	
8	3 to 4 _ T125	$\begin{pmatrix} s_{33} & s_{34} \\ s_{43} & s_{44} \end{pmatrix}$	3	
9	3 to 5 _ T124	$\begin{pmatrix} s_{33} & s_{35} \\ s_{53} & s_{55} \end{pmatrix}$	10	
10	4 to 5 _ T123	$\begin{pmatrix} s_{44} & s_{45} \\ s_{54} & s_{55} \end{pmatrix}$	4	

Table D.3: Measurement combinations of a 5-port network using a 2-port VNA

## D.4 6-Port Network Measurements

Number of measurements required: 15

#	Measurement	Partial S-Matrix	Insert Order into GUI (B.5)	Reconstructed S-Matrix
1	1 to 2 _ T3456	$\begin{pmatrix} s_{11} & s_{12} \\ s_{21} & s_{22} \end{pmatrix}$	1	$\begin{pmatrix} s_{11} & s_{12} & s_{13} & s_{14} & s_{15} & s_{16} \\ s_{21} & s_{22} & s_{23} & s_{24} & s_{25} & s_{26} \\ s_{31} & s_{32} & s_{33} & s_{34} & s_{35} & s_{36} \\ s_{41} & s_{42} & s_{43} & s_{44} & s_{45} & s_{46} \\ s_{51} & s_{52} & s_{53} & s_{54} & s_{55} & s_{56} \\ s_{61} & s_{62} & s_{63} & s_{64} & s_{65} & s_{66} \end{pmatrix}$
2	1 to 3 _ T2456	$\begin{pmatrix} s_{11} & s_{13} \\ s_{31} & s_{33} \end{pmatrix}$	6	
3	1 to 4 _ T2356	$\begin{pmatrix} s_{11} & s_{14} \\ s_{41} & s_{44} \end{pmatrix}$	7	
4	1 to 5 _ T2346	$\begin{pmatrix} s_{11} & s_{15} \\ s_{51} & s_{55} \end{pmatrix}$	8	
5	1 to 6 _ T2345	$\begin{pmatrix} s_{11} & s_{16} \\ s_{61} & s_{66} \end{pmatrix}$	9	
6	2 to 3 _ T1456	$\begin{pmatrix} s_{22} & s_{23} \\ s_{32} & s_{33} \end{pmatrix}$	2	
7	2 to 4 _ T1356	$\begin{pmatrix} s_{22} & s_{24} \\ s_{42} & s_{44} \end{pmatrix}$	10	
8	2 to 5 _ T1346	$\begin{pmatrix} s_{22} & s_{25} \\ s_{52} & s_{55} \end{pmatrix}$	11	
9	2 to 6 _ T1345	$\begin{pmatrix} s_{22} & s_{26} \\ s_{62} & s_{66} \end{pmatrix}$	12	
10	3 to 4 _ T1256	$\begin{pmatrix} s_{33} & s_{34} \\ s_{43} & s_{44} \end{pmatrix}$	3	
11	3 to 5 _ T1246	$\begin{pmatrix} s_{33} & s_{35} \\ s_{53} & s_{55} \end{pmatrix}$	13	
12	3 to 6 _ T1245	$\begin{pmatrix} s_{33} & s_{36} \\ s_{63} & s_{66} \end{pmatrix}$	14	
13	4 to 5 _ T1236	$\begin{pmatrix} s_{44} & s_{45} \\ s_{54} & s_{55} \end{pmatrix}$	4	
14	4 to 6 _ T1235	$\begin{pmatrix} s_{44} & s_{46} \\ s_{64} & s_{66} \end{pmatrix}$	15	
15	5 to 6 _ T1234	$\begin{pmatrix} s_{55} & s_{56} \\ s_{65} & s_{66} \end{pmatrix}$	5	

Table D.4: Measurement combinations of a 6-port network using a 2-port VNA

# E Documentation of the Master Thesis on CD

The attached CD contains

- the Master Thesis in PDF format
- the literature used